Journal Pre-proof

Design, synthesis and antitumor evaluation of new 1,8-naphthalimide derivatives targeting nuclear DNA

Gui-Bin Liang, Jian-Hua Wei, Hong Jiang, Ri-Zhen Huang, Jing-Ting Qin, Hui-Ling Wang, Heng-Shan Wang, Ye Zhang

PII: S0223-5234(20)30923-5

DOI: https://doi.org/10.1016/j.ejmech.2020.112951

Reference: EJMECH 112951

To appear in: *European Journal of Medicinal Chemistry*

Received Date: 23 August 2020

Revised Date: 15 October 2020

Accepted Date: 15 October 2020

Please cite this article as: G.-B. Liang, J.-H. Wei, H. Jiang, R.-Z. Huang, J.-T. Qin, H.-L. Wang, H.-S. Wang, Y. Zhang, Design, synthesis and antitumor evaluation of new 1,8-naphthalimide derivatives targeting nuclear DNA, *European Journal of Medicinal Chemistry*, https://doi.org/10.1016/j.ejmech.2020.112951.

Graphical abstract

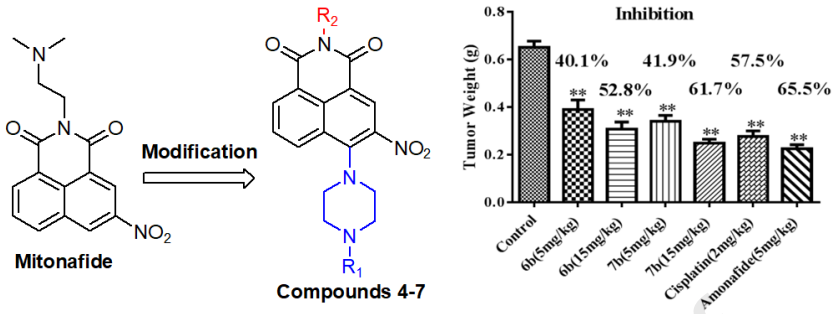

Design, synthesis and antitumor evaluation of new 1,8-naphthalimide derivatives targeting nuclear DNA

Gui-Bin Liang[a,b,†], Jian-Hua Wei[a,†,*], Hong Jiang[a,†], Ri-Zhen Huang[a,b], Jing-Ting Qin[a], Hui-Ling Wang[a], Heng-Shan Wang[b], Ye Zhang[a,c,d,*]

[a]*School of Pharmacy, Guilin Medical University, Guilin 541004, China*

[b]*State Key Laboratory for Chemistry and Molecular Engineering of Medicinal Resources, School of Chemistry and Pharmacy, Guangxi Normal University, Guilin 541004, China*

[c]*Department of Chemistry & Pharmaceutical Science, Guilin Normal College, Guilin 541001, China*

[d]*College of Chemistry and Food Science, Yulin Normal University, Yulin 537000, China*

[†]These authors contributed equally to this work.

[*]Corresponding author. School of Pharmacy, Guilin Medical University, Guilin 541004, China

Tel: (086) 773−2120998; fax: (086) 773−21209958

E-mail addresses: zhangye81@126.com (Y. Zhang), 352142863@qq.com (J.-H Wei)

Abstract

Four series of new 3-nitro naphthalimides derivatives, **4**(**4a**–**4f**), **5**(**5a**–**5i**), **6**(**6a**–**6e**) and **7**(**7a**–**7j**), were designed and synthesized as antitumor agents. Methyl thiazolyl tetrazolium (MTT) screening assay results revealed that some compounds displayed effective *in vitro* antiproliferative activity on SMMC-7721, T24, SKOV-3, A549 and MGC-803 cancer cell lines in comparison with 5-fluorouracil (5-FU), mitonafide and amonafide. Nude mouse xenotransplantation model assay results indicated that compounds **6b** and **7b** exhibited good *in vivo* antiproliferative activity in MGC-803 xenografts in comparison with amonafide and cisplatin, suggesting that compounds **6b** and **7b** could be good candidates for antitumor agents. Gel electrophoresis assay indicated that DNA and Topo I were the potential targets of compounds **6b** and **7b**, and comet assay confirmed that compounds **6b** and **7b** could induce DNA damage, while the further study showed that the **6b**- and **7b**-induced DNA damage was accompanied by the upregulation of p-ATM, P-Chk2, Cdc25A and p-H2AX. Cell cycle arrest studies demonstrated that compounds **6b** and **7b** arrested the cell cycle at the S phase, accompanied by the upregulation of the expression levels of the antioncogene p21 and the down-regulation of the expression levels of cyclin E. Apoptosis assays indicated that compounds **6b** and **7b** caused the apoptosis of tumor cells along with the upregulation of the expression of Bax, caspase-3, caspase-9 and PARP and the downregulation of Bcl-2. These mechanistic studies suggested that compounds **6b** and **7b** exerted their antitumor activity by targeting to DNA, thereby inducing DNA damage and Topo I inhibition, and consequently causing S stage arrest and the induction of apoptosis.

Keywords: naphthalimide derivatives; antitumor activity; DNA damage; Topo I inhibition; cell cycle arrest and apoptosis

1. Introduction

Carcinoma is a disease of global importance and is caused by abnormal and uncontrolled cell division and growth in an undesired manner. DNA plays an essential role in the uncontrolled cell division and growth and is thus considered as a viable target for chemotherapy[1]. Many chemotherapy drugs exert their anticancer activities by targeting DNA, thereby causing DNA damage and DNA topoisomerase (Topo I and/or II) inhibition and consequently activating cell cycle checkpoint and apoptosis responses[1-4]. Mitonafide is a typical DNA-targeting naphthalimide chemotherapy agent and has entered clinical trials[5]. However, serious adverse toxic side effects have limited further clinical trials[5,6]. In order to improve this problem, many structural modifications of the naphthalimide skeleton, including the modification at the *N*-position and positions 3 and 4 in the naphthalimide moiety, have been described in the literature[5,7-11]. And the introduced nitro moiety at 3 position has been proved to be a typical substituent preferably for the antitumor activity[5-11].

Characterized by a planar π-deficient chromophore system, naphthalimides are a promising class of DNA-targeted anticancer compounds that exhibit potent antitumor activities and effectively inhibit tumor growth[6,12]. Mitonafide (Fig. 1) is a leading member of this family that effectively targets DNA and has entered clinical trials, though its severe toxicity has seriously hampered further application. In addition, mitonafide has been proven to be metabolized into amonafide (Fig. 1) in physiological environments[13], while amonafide could be finally acetylated and converted to a toxic amino-acetyl metabolite by *N*-acetyl-transferase 2[6,12]. To improve its antitumor activity and reduce its adverse toxicity, much attention has been paid to the structural modification of mitonafide. It is recognized that modifications at the *N*-position in the cyclic imide ring and at the 4-position in the mitonafide moiety have considerable influence on the antitumor effect, toxicity and intercalation with DNA, according to the study of structure-activity relationships of numerous 1,8-naphthalimide derivatives, while in some cases even a small modification may lead to a vital effect on their antitumor activity[5,7,9,10,11,14].

Piperazine and its substitution derivatives are considered as privileged scaffolds in drug discovery and widely introduced in many antitumor drugs, such as palbociclib, nintedanib esylate, olmutinib and entrectinib. So, it is believed that piperazine derivatives may exhibit potent anticancer activities; our previous work has demonstrated that the introduction of piperazine scaffolds to some pharmacy core could improve the antitumor activity and the toxicity of its analogs[15,16]. Therefore, the modification of antitumor pharmacy cores with piperazine structures has attracted much attention among medicinal chemists.

Encouraged by the antitumor and DNA-targeting activity of mitonafide and the virtues of piperazine structures, it is expected that the combination of piperazine scaffolds and mitonafide may improve antitumor efficiency and toxicity. Therefore, as the continuation of our previous work[17], different substituent groups fused were introduced in the functional piperazine moiety

at the 4-position of the mitonafide moiety in the present work, while some other substituents at the *N*-position of the imide ring were also designed and used for comparison (Fig. 1). We expected that the introduction of piperazine scaffolds at 4-position of mitonafide could trigger steric hindrance effect and slow down its metabolism into amonafide, thereby improving the antitumor efficiency and toxicity. With this expectation in mind, the target compounds, their antiproliferative activity and the antitumor mechanisms related to DNA-targeting were investigated.

[Fig. 1]

2. Results and discussion

2.1. Chemistry

The synthetic route leading to the target 1,8-naphthalimide derivatives **4**−**7** is outlined in Scheme 1 and Scheme 2. First, as shown in Scheme 1, the benzoylation and sulfonylation of *N*-Boc piperazine (**NBP**) with benzoyl chloride and p-toluenesulfonyl chloride at room temperature yielded *N*-boc-*N*-benzoyl piperazine (**NBNBZP**) and *N*-boc-*N*-p-toluenesulfonyl piperazine (**NBNTP**), respectively, in accordance with previous studies[18,19], while the treatment of **NBP** with carbon disulfide, potassium carbonate and benzyl bromide in the presence of dichloromethane for 2 h offered *N*-boc-*N*-benzyl dithioformyl piperazine (**NBNBDP**) in good yield, in an ice-water bath. These three intermediates **NBNBZP**, **NBNTP** and **NBNBDP** were then hydrolyzed with trifluoroacetica acid (TFA) to offer *N*-benzoyl piperazine (**NBZP**), *N*-p-toluenesulfonyl piperazine (**NTP**) and *N*-benzyl dithioformyl piperazine (**NBDP**) at good yield, respectively[18,19]. Secondly, as shown in Scheme 2, the treatment of 4-bromo-1,8-naphthalic anhydride (**1**) with $NaNO_3$ and H_2SO_4 at 0°C offered 3-nitro-4-bromo-naphthalic anhydride (**2**) in good yield, in accordance with our previous work[17]. Then the four *N*-substituted piperazines **NBP**, **NBDP**, **NBZP** and **NTP** were treated with compound **2** in the presence of 2-methoxyethanol at 110°C to provide 4-piperazine-3-nitro-1,8-naphthalic anhydride **3a–3d** in moderate yield, respectively. Finally, the desired 1,8-naphthalimides **4a–4f**, **5a–5i**, **6a–6e** and **7a–7j** were obtained in moderate yield, by the condensation of primary amines with **3a–3d** at 80°C in the presence of ethanol, respectively.

[**Scheme 1**]

[**Scheme 2**]

The chemical structures of these desired compounds **4a–4f**, **5a–5i**, **6a–6e** and **7a–7j** were then confirmed by ^{1}H NMR, ^{13}C NMR and high resolution mass spectrometry (HR-MS) (see Part 2 of Supplementary Data). In the ^{1}H NMR spectra for compounds **4a–4f**, **5a–5i**, **6a–6e** and **7a–7j**, the chemical shift (δ) around 8.85−6.48 was attributed to the aromatic hydrogens (H-Ar) fused in naphthalimide and aromatic rings, while δ in the range of 4.09−3.21 was mainly ascribed to the

hydrogens of the piperazine ring. In ^{13}C NMR spectra, δ in the range of 160−165 was mainly attributed to the carbons in carbonyl groups, and δ around 46 and 51 was ascribed to the carbons in the piperazine moiety, while δ in the range of 185−189 was attributed to the carbon in the thiocarbonyl group. In addition, HR-MS results for **4a–4f**, **5a–5i**, **6a–6e** and **7a–7j** were also consistent with their chemical structures in Scheme 2. Hence, the chemical structures of compounds **4a–4f**, **5a–5i**, **6a–6e** and **7a–7j** were identified.

2.2. Antitumor activity

2.2.1. In vitro antiproliferative activity

With these target compounds at hand, we investigated their antiproliferative activity by MTT[15-17] against human liver cancer SMMC-7721 cells, human bladder cancer T24 cells, human ovarian cancer SKOV3 cells, human hepatoma A549 cells and human gastric cancer MGC-803 cells, using 5-FU, mitonafide and amonafide as the positive controls.

As shown in Table 1, most of the target compounds exhibited evident *in vitro* antiproliferative activity on these five cell lines. Table 1 shows that in the inhibition assay with SMMC-7721 cells, most compounds (except for compounds **4e**, **5a**, **5e**, **6e**, **7a**, **7c**, **7d** and **7j**) exhibited better antiproliferative activity than the commercial anticancer drug 5-FU (IC_{50} = 15.32 ± 0.67 μM), and compounds **4a**, **4b**, **5b**, **6a**, **6b** and **7b** displayed higher antiproliferative activity than amonafide (IC_{50} = 6.93 ± 0.26 μM). Importantly, compounds **4b**, **6b** and **7b** even showed more potent antiproliferative activity than mitonafide (IC_{50} = 3.22 ± 0.26 μM), with IC_{50} values of 1.05 ± 0.09 μM, 1.57 ± 0.19 μM and 2.71 ± 0.13 μM, respectively, indicating that compounds **4b**, **6b** and **7b** exhibited potent antiproliferative activity against this cell line. In the antiproliferation assay with T24 cells, all the target compounds **4–7** exhibited better antiproliferative activity than 5-FU (IC_{50} = 40.14 ± 2.14 μM), and compounds **4a**, **4b**, **5b**, **6a**, **6b** and **7b** demonstrated better antiproliferative activity than amonafide (IC_{50} = 5.01 ± 0.47 μM), while **4b**, **6b** and **7b** showed more potent antiproliferation than mitonafide (IC_{50} = 1.11 ± 0.31 μM), with IC_{50} values of 0.83 ± 0.15 μM, 0.42 ± 0.05 μM and 0.33 ± 0.07 μM, respectively, indicating their favorable antiproliferation on this cell line. In the SKOV3 assay, many compounds (except for **5a**, **5c**, **5d**, **5g–5i**, **7d** and **7g–7j**) exhibited better antiproliferative activity than 5-FU (IC_{50} = 26.34 ± 0.57 μM), and compounds **4b**, **5b**, **6a**, **6b** and **7b** displayed stronger antiproliferative activity than amonafide (IC_{50} = 6.31 ± 0.46 μM), while compounds **4b** and **7b** exhibited better antiproliferation than mitonafide (IC_{50} = 1.38 ± 0.51 μM), with IC_{50} values of 0.65 ± 0.13 μM and 0.32 ± 0.03 μM, respectively, demonstrating the strong antiproliferative effects of compounds **4b** and **7b** against SKOV3 cells. In the A549 test, except for compounds **4c–4e**, **5a**, **5h**, **5i**, **6d**, **7d** and **7f–7j**, other compounds showed stronger antiproliferation activity than 5-FU (IC_{50} = 34.47 ± 1.90 μM), while compounds **4a**, **4b**, **5b**, **6a**, **6b** and **7b** displayed stronger antiproliferation activity than amonafide

(IC_{50} = 7.94 ± 0.61 μM), with IC_{50} values of 1.08 ± 0.15 μM, 7.52 ± 0.36 μM, 1.98 ± 0.11 μM, 6.66 ± 0.23 μM, 0.41 ± 0.12 μM and 0.27 ± 0.15 μM, respectively. Unfortunately, no compound showed better antiproliferation activity than mitonafide in this cell line. In the MGC-803 cell assay, all these compounds exhibited better antiproliferative activity than 5-FU (IC_{50} = 34.85 ± 1.75 μM), and compounds **4a**, **4b**, **4e**, **5b**, **6a**, **6b** and **7b** exhibited higher antiproliferative activity than amonafide (IC_{50} = 9.06 ± 0.45 μM), while compounds **4a**, **4b**, **5b**, **6b** and **7b** even showed more potent antiproliferative activity than mitonafide (IC_{50} = 6.80 ± 0.45 μM), with IC_{50} values of 1.33 ± 0.23 μM, 6.44 ± 0.12 μM, 6.08 ± 0.21 μM, 0.868 ± 0.16 μM and 1.42 ± 0.11 μM, respectively, indicating that compounds **4a**, **4b**, **5b**, **6b** and **7b** exhibited potent antiproliferative activity against this cell line. On the basis of the above MTT results, compounds **6b** and **7b** displayed the best antiproliferative activity on these five cell lines, and were thus chosen as representative compounds for further investigation of the *in vivo* antiproliferative activity.

[**Table 1**]

In addition, based on the MTT results, some interesting structure-activity relationships may be concluded: (1) both of the substituent groups at the *N*-position in the cycloamidite moiety and the 4-position had important but irregular influences on the antiproliferative activity; (2) importantly, the fatty chain amine *N*,*N*-dimethylaminoethyl at the *N*-position in the cycloamidite ring showed especially positive effects on the antiproliferative activity; (3) the comparison of **4** with **5**, **6** and **7**, demonstrated that substitution in the piperazine moiety exhibited important but irregular effect on their antiproliferative activity, while the aliphatic chain hydrocarbon may have positive effects on the antiproliferative activity. This result indicated that in some cases even a small structural transformation in the 1,8-naphthalimide skeleton may have a major effect on their antitumor activity, well consistent with previous literature[6,17].

2.2.2 In vivo antiproliferative activity

To further evaluate the antitumor activity of **6b** and **7b**, *in vivo* antiproliferation assays were performed. The MGC-803 xenograft model was chosen in this study, based on the *in vitro* antiproliferation experimental result. Specific pathogen-free BALB/c nude mice were divided randomly into five groups, i.e., the vehicle control group, the low-dose and high-dose administration of compounds **6b** and **7b** groups and two positive control groups. Saline, low dose (5 mg/kg) and high dose (15 mg/kg) compounds **6b** and **7b**, cisplatin (2 mg/kg) and amonafide (5 mg/kg) were administrated by intraperitoneal injection. The relative tumor increment rate (T/C) and tumor inhibitory rate (IR) were then calculated to assess their *in vivo* antitumor activity, where T/C values of less than 60.0% and IR values of more than 40.0% indicated potent and effective antitumor activity[20].

[Fig. 2]

As shown in Fig. 2A, administration of **6b** and **7b**, at both low (5 mg/kg) and high doses (15 mg/kg), had strong antiproliferative effects on MGC-803 tumor growth; and the T/C values were 59.8% (**6b** at low dose), 47.1% (**6b** at high dose), 52.0% (**7b** at low dose) and 38.4% (**7b** at high dose). In comparison, cisplatin (2 mg/kg) and amonafide (5 mg/kg) had T/C values of 42.3% and 34.4%, respectively. The tumors of the mice were collected (Fig. 2B) and weighed on day 21 to assess the antiproliferative rates based on the increase in tumor weight. As shown in Fig. 2D, compounds **6b** and **7b** displayed obvious antitumor activity in the MGC-803 model with inhibitory rates of 40.1% (**6b** at low dose), 52.8% (**6b** at high dose), 41.9% (**7b** at low dose) and 61.7% (**7b** at high dose), while those of cisplatin (2 mg/kg) and amonafide (5 mg/kg) were 57.5% ($P < 0.01$) and 65.5% ($P < 0.01$), respectively. Compounds **6b** and **7b** at both low and high doses displayed T/C values of less than 60.0% and IR values of more than 40.0% and strong *in vivo* antiproliferative effects in comparison with cisplatin and amonafide, demonstrating that compounds **6b** and **7b** displayed effective antitumor activity in MGC-803 xenografts. Interestingly, as shown in Fig. 2C, no obvious adverse effects and changes in body weight were found in the mice treated with compounds **6b** and **7b**, indicating that **6b** and **7b** had no significant toxicity to mice within the 21-day period of treatment and thus could be good candidates for antitumor drug design. The high administration doses of **6b** and **7b** may also indirectly indicate their lower toxicity in comparison with cisplatin and amonafide.

2.3 Antitumor mechanism investigation

2.3.1. DNA intercalation

Because a planar chromophore portion is considered as the common feature of DNA-intercalating anticancer drugs, it is reasonable that DNA is and has been proven as the potential target for naphthalimide derivatives[5]. To obtain insight into the mechanism of naphthalimide derivatives targeting DNA, a gel electrophoresis assay was carried out, using mitonafide and amonafide as positive controls. Gel electrophoresis assay results (Fig. 3) indicated that **6b** and **7b** tightly bound to the supercoiled circular plasmid pBR322 and hindered its migration in the gel at concentrations from 10 μM to 100 μM, while they displayed no photocleavage activity or photoreactivity in this assay, confirming that compound **6b** and **7b** exhibited important intercalation effects on pBR322.

[Fig. 3]

To better understand the intercalation effects of compounds **6b** and **7b** with DNA, we performed molecular docking studies using SYBYL-X 2.0 software. As shown in Fig. S1-1, compounds **6b** and **7b** stacked with the regions of the DNA minor groove by surface binding

interactions and adjunction with the target DNA double helix, implying their good binding affinity with DNA. It was obvious that compounds **6b** and **7b** intercalated with nucleotide and forming hydrogen bonds with NH group presented at DNA. Therefore, the results could confer the anticancer activity of compounds **6b** and **7b** to their abilities to bind to DNA minor groove.

2.3.2. DNA damage

To investigate whether compounds **6b** and **7b** could lead to DNA damage, a comet assay, which was proven to be a sensitive, simple but useful tool for DNA damage studies[21], was performed. As shown in Fig. 4, long DNA tails were found after treatment with compounds **6b** and **7b**, indicating compounds **6b** and **7b** could induce DNA damage[21].

[Fig. 4]

It is believed that PIKK kinases (ATM, ATR and DNA-PK), mediator or signal transducer proteins (Chk1 and Chk2 signaling kinases) and effector proteins (phosphatases Cdc25A/B/C and cyclin-dependent kinases [CDKs]) are main regulators of the DNA damage response and play an important role in the course of DNA damage[2], while the increased levels of human p-H2AX are considered as important evidence of DNA damage[22,23]. Hence, the expression levels of p-ATM, P-Chk2, Cdc25A and p-H2AX in MGC-803 cells were examined by western blots. The results (Fig. 5) show that compared to the control, the expression levels of p-ATM, P-Chk2, Cdc25A and p-H2AX were significantly upregulated in MGC-803 cells treated with **6b** and **7b**, directly verifying the presence of damaged DNA.

[Fig. 5]

2.3.3. Topo I inhibition

To study whether the inhibition of Topo 1 activity was related to the antiproliferative and DNA-damaging effects of **6b** and **7b**, the DNA relaxation assay was carried out using amonafide, mitonafide and the Topo I inhibitor camptothecin (CPT) as positive controls. The results (Fig. 6 and Fig. S1-2) indicate that, accompanying the DNA damage, compound **7b** exhibited obvious Topo I inhibition (0.1 U/L) at a concentration of 20 μM, while compound **6b** exhibited evident Topo I inhibition (0.1 U/L) at a concentration of 10 μM, implying that in addition to DNA, Topo I was also a potential target of compounds **6b** and **7b**. To further determine the DNA relaxation induced by compounds **6b** and **7b**, an unwinding assay was then carried out. The results (Fig. S1-3 and Fig. S1-4) show that compounds **6b** and **7b** exhibited obvious Topo I inhibition at low concentrations (< 20 μM), while they led to the supercoiling of DNA at high concentrations (> 40 μM), confirming that DNA and Topo I are indeed potential targets of compounds **6b** and **7b**.

[Fig. 6]

2.3.4 Cell cycle arrest analysis

Because DNA-targeted drugs can usually induce cell cycle arrest[2], the effects of compounds **6b** and **7b** on cell cycle progression were investigated. As shown in Fig. 7, in MGC-803 cells, compounds **6b** and **7b** mainly arrested the cell cycle at the S phase, causing an evident increase in the S phase population (for **6b**: 37.80% at 0.25 μM, 69.18% at 0.5 μM and 71.16% at 1 μM; for **7b**: 40.44% at 0.25 μM, 43.96% at 0.5 μM and 75.18% at 1 μM) in comparison with the control group (20.23%).

[Fig. 7]

The regulatory proteins CDK and cyclin E and the antioncogene p21 play an important role in the regulation of the S phase checkpoint[23]. Therefore, the expression of CDK2, cyclin E and p21 in MGC-803 cells was examined by western blots, using glyceraldehyde-3-phosphate dehydrogenase (GAPDH) as a control. As shown in Fig. 8, treatment with compounds **6b** and **7b** increased p21 expression, decreased cyclin E expression and only slightly affected CDK2 expression, indicating that compounds **6b** and **7b** induced S phase cell cycle arrest by inhibiting the S phase-promoting CDK2–Cyclin E complex in MGC-803 cells[22].

[Fig. 8]

2.3.5 Apoptosis study

To further assess the antitumor mechanism of compounds **6b** and **7b**, apoptosis levels were investigated. As shown in Fig. 9, in MGC-803 cells, **6b** increased the percentage of apoptotic cells to 21.7%, 28.7% and 52.5% (including the early and late apoptosis) at 0.25, 0.5 and 1 μM, respectively, while **7b** increased the percentage of apoptotic cells to 17.3%, 22.9% and 27% at the same concentrations, indicating that compounds **6b** and **7b** could induce apoptosis in MGC-803 cells.

[Fig. 9]

Bcl-2/Bax family proteins, caspase proteases and poly(ADP-ribose) polymerase (PARP) play important mediating roles in apoptosis[24-26]. To further study the mechanisms underlying **6b**- and **7b**-induced apoptosis, the expression levels of Bax, Bcl-2, caspase-9, caspase-3 and PARP in MGC-803 cells treated with compounds **6b** and **7b** were measured by western blot. The results (Fig. 10) indicated that compounds **6b** and **7b** could upregulate the expression levels of Bax, caspase-3, caspase-9 and PARP and downregulate Bcl-2 levels, implying that compounds **6b** and **7b** may exert proapoptotic effects through a mitochondrial-mediated pathway and a caspase cascade.

[Fig. 10]

3. Conclusion

In this study, we designed and synthesized four sets of naphthalimide derivatives and evaluated their antitumor activity against five cancer cell lines, i.e., SMMC-7721, T24, SKOV-3, A549 and MGC-803. We identified some compounds displaying high *in vitro* antitumor activity in comparison with 5-FU, mitonafide and amonafide, while compounds **6b** and **7b** displayed good *in vivo* antitumor activity in the MGC-803 xenograft in comparison with amonafide and cisplatin. Our gel electrophoresis assay indicated that DNA and Topo I are potential targets of compounds **6b** and **7b**, and our comet assay confirmed that compounds **6b** and **7b** could induce DNA damage, while the further study showed that the **6b**- and **7b**-induced DNA damage was accompanied by the upregulation of p-ATM, P-Chk2, Cdc25A and p-H2AX. Cell cycle arrest studies demonstrated that compounds **6b** and **7b** trigger cell cycle arrest at the S phase through inhibition of CDK2–Cyclin E complex activity, while apoptosis assays indicated that compounds **6b** and **7b** could cause the apoptosis of tumor cells along with the upregulation of the expression Bax, caspase-3, caspase-9 and PARP and downregulation of Bcl-2. Based on these observations, it could be concluded that compounds **6b** and **7b** may mainly exert their antitumor effects by targeting to DNA, thereby inducing DNA damage and inhibiting Topo I, and consequently causing to S phase arrest and inducing apoptosis.

4. Experimental procedures

4.1 Materials and instruments

All chemicals and solvents were of reagent grade and purchased from Aladdin (Shanghai) and used without further purification. The materials used for biological experiments with pBR322 DNA and cell lines were purchased from Aladdin, Topo I was purchased from TaKaRa Biotechnology Co., Ltd. (Dalian), and antibodies were purchased from Cell Signaling Technology. Cell cycle and apoptosis assays were performed by BD FACSAria III flow cytometry (Becton Dickinson) and the results were analyzed by ImageJ software. The NMR spectra were measured on a BRUKER AVANCE AV 400/600 instrument, while the mass spectra were examined on a BRUKER ESQUIRE HCT spectrometer.

4.2. Chemistry: general synthesis procedure for compounds 4−7

NBP was purchased form Aladdin and the intermediate compounds **ZBZP**, **NTP** and **NBDP** were synthesized as previously described[18,19], using **NBP** as the starting material. The mixture of compound **2** (1.5 mmol), the prefabricated 1-tosylpiperazine (**NBP**, **ZBZP**, **NTP** and **NBDP**)

(1.8 mmol) and ethylene glycol methyl ether (100 mL) was reacted at 110°C for 8 h. After the reaction, the reaction solution was cooled naturally overnight and then filtered to provide desired compounds **3** (**3a–3d**). Compounds **3** (**3a–3d**) were then purified by silica column chromatography, using dichloromethane–methanol (v:v = 10:1) solution as the eluent. Finally, compounds **3** (**3a–3d**) (1.0 mmol) were treated with the primarily amines (1.0 mmol) in hot ethanol at 80°C for 6 h. The reaction solutions were cooled naturally overnight and then filtered to offer the target compounds **4a–4f**, **5a–5i**, **6a–6e** and **7a–7j**. Compounds **4–7** were purified by silica column chromatography, using dichloromethane–methanol (v:v = 8:1) solution as the eluent.

***Tert-butyl 4-(2-(3-(methylamino)propyl)-5-nitro-1,3-dioxo-2,3-dihydro-1H-benzo[de]isoquinolin-6-yl)piperazine-1-carboxylate (4a)*:** Yellow solid, yield 42.7%. ^{1}H NMR (400 MHz, DMSO-d_6) δ 8.67 – 8.62 (m, 1H, H-Ar), 8.56 (dd, *J* = 7.2, 0.7 Hz, 1H, H-Ar), 8.52 (s, 1H, H-Ar), 7.99 – 7.92 (m, 1H, H-Ar), 4.04 (t, *J* = 7.2 Hz, 2H, -CH_2), 3.66 (s, 4H, 2-CH_2), 3.18 (d, *J* = 4.6 Hz, 5H, 2-CH_2), 2.60 – 2.57 (m, 2H, -CH_2), 2.29 (s, 3H, -CH_3), 1.82 – 1.71 (m, 2H, -CH_2), 1.45 (s, 9H, 3-CH_3).^{13}C NMR (100 MHz, DMSO-d_6) δ 162.95 (C=O), 161.84 (C=O), 153.98, 147.01, 142.23, 132.80, 131.45, 129.58, 129.06, 128.48, 126.30, 122.98, 117.75, 79.30 (C-O), 51.06 (C-N), 48.60 (CH_2), 45.41(C-N), 38.11(CH_3), 35.43(CH_2), 28.03(CH_3), 27.02(CH_2). HRMS (m/z) (ESI): $C_{25}H_{31}N_5O_6$ $[M+1]^+$ calcd for: 498.2269, found: 498.2335.

***Tert-butyl 4-(2-(2-(dimethylamino)ethyl)-5-nitro-1,3-dioxo-2,3-dihydro-1H-benzo[de]isoquinolin-6-yl)piperazine-1-carboxylate (4b)*:** Yellow solid, yield 47.4%. ^{1}H NMR (400 MHz, DMSO-d_6) δ 8.67 (d, *J* = 8.5 Hz, 1H, H-Ar), 8.59 (d, *J* = 7.2 Hz, 1H, H-Ar), 8.56 (s, 1H, H-Ar), 8.02 – 7.94 (m, 1H, H-Ar), 4.13 (t, *J* = 6.8 Hz, 2H, -CH_2), 3.66 (s, 4H, 2-CH_2), 3.19 (d, *J* = 4.0 Hz, 4H, 2-CH_2), 2.29 (s, 2H, -CH_2), 2.20 (s, 6H, 2-CH_3), 1.45 (s, 9H, 3-CH_3).^{13}C NMR (100 MHz, DMSO-d_6) δ 162.92 (C=O), 161.79 (C=O), 153.99, 147.09, 142.29, 132.91, 131.55, 129.60, 129.14, 128.51, 126.44, 122.93, 117.68, 79.30 (C-O), 56.35 (CH_3), 51.06 (C-N), 45.36 (CH_2), 37.71 (CH_2), 28.04 (CH_3). HRMS (m/z) (ESI): $C_{25}H_{31}N_5O_6[M+1]^+$ calcd for: 498.2347, found: 498.2330.

***Tert-butyl 4-(2-(2-hydroxyethyl)-5-nitro-1,3-dioxo-2,3-dihydro-1H-benzo[de]isoquinolin-6-yl)piperazine-1-carboxylate (4c)*:** Yellow solid, yield 48.1%. ^{1}H NMR (400 MHz, DMSO-d_6) δ 8.60 (dd, *J* = 8.4, 0.8 Hz, 1H, H-Ar), 8.51 (dd, *J* = 7.4, 0.8 Hz, 1H, H-Ar), 8.47 (s, 1H, H-Ar), 7.92 (dd, *J* = 8.4, 7.4 Hz, 1H, H-Ar), 4.79 (t, *J* = 5.9 Hz, 1H, -OH), 4.08 (t, *J* = 6.5 Hz, 2H, -CH_2), 3.66 (s, 4H, 2-CH_2), 3.61 – 3.56 (m, 2H, -CH_2), 3.22 – 3.08 (m, 4H, 2-CH_2), 1.46 (s, 9H, 3-CH_3).^{13}C NMR (100 MHz, DMSO-d_6) δ 162.90 (C=O), 161.79 (C=O), 153.98, 146.90, 142.13, 132.71, 131.30, 129.47, 128.94, 128.42, 126.18, 122.95, 117.71, 79.30 (C-O), 57.64 (CH_2-OH), 51.05 (C-N), 41.91(CH_2), 28.03 (CH_3).HRMS (m/z) (ESI):$C_{23}H_{26}N_4O_7[M+Na]^+$ calcd for: 493.1694, found: 493.1679.

***Tert-butyl 4-(2-(4-chlorobenzyl)-5-nitro-1,3-dioxo-2,3-dihydro-1H-benzo[de]isoquinolin-6-yl)piperazine-1-carboxylate (4d)*:** Yellow solid, yield 46.4%. ^{1}H NMR (400 MHz, DMSO-d_6) δ 8.66 (d, *J* = 8.4 Hz, 1H, H-Ar), 8.58 (d, *J* = 7.2 Hz, 1H, H-Ar), 8.55 (s, 1H, H-Ar), 7.96 (dd, *J* = 8.4, 7.2 Hz, 1H, H-Ar), 7.35 (q, *J* = 8.7 Hz, 4H, H-Ar), 5.18 (s, 2H, -CH_2), 3.66 (s, 4H, 2-CH_2), 3.23 – 3.11 (m, 4H, 2-CH_2), 1.45 (s, 9H, 3-CH_3).^{13}C NMR (100 MHz, DMSO-d_6) δ 162.97 (C=O), 161.86 (C=O), 153.97, 147.24, 142.21, 136.01, 133.07, 131.73, 129.71, 129.51, 129.08, 128.49, 128.27, 126.67, 122.81, 117.47, 79.29 (C-O), 51.10 (C-N), 42.41 (CH_2), 28.02 (CH_3). HRMS (m/z) (ESI): $C_{28}H_{27}ClN_4O_6[M+Na]^+$ calcd for: 573.1511, found: 573.1490.

***Tert-butyl 4-(2-(3,4-dihydroxyphenethyl)-5-nitro-1,3-dioxo-2,3-dihydro-1H-benzo[de]isoquinolin-6-yl)piperazine-1-carboxylate (4e)*:** Yellow solid, yield 44.4%. ^{1}H NMR (400 MHz, DMSO-d_6) δ 8.79 (s, 1H, -OH), 8.70 – 8.61 (m, 2H, H-Ar), 8.57 (d, *J* = 0.7 Hz, 1H, H-Ar), 8.53 (s, 1H,-OH), 7.95 (dd, *J* = 8.4, 7.4 Hz, 1H, H-Ar), 6.63 (dd, *J* = 11.0, 5.0 Hz, 2H, H-Ar), 6.47 (dd, *J* = 8.0, 2.0 Hz, 1H, H-Ar), 4.12 (dd, *J* = 8.9, 6.8 Hz, 2H, -CH_2), 3.66 (s, 4H, 2-CH_2), 3.25 – 3.08 (m, 4H, 2-CH_2), 2.77 – 2.63 (m, 2H, -CH_2), 1.46 (s, 9H, 3-CH_3).^{13}C NMR (100 MHz, DMSO-d_6) δ 162.73 (C=O), 161.61 (C=O), 153.98, 147.06, 145.16, 143.73, 142.20, 132.82, 131.49, 129.54, 129.27, 129.07, 128.48, 126.33, 122.91, 119.21, 117.64, 115.93, 115.58, 79.30 (C-O), 51.07 (C-N), 41.48 (CH_2), 32.80 (CH_2), 28.04 (CH_3). HRMS (m/z) (ESI): $C_{29}H_{30}N_4O_8[M+Na]^+$ calcd for: 585.1956, found: 585.1934.

***Tert-butyl 4-(2-(2-(benzo[d][1,3]dioxol-5-yl)ethyl)-5-nitro-1,3-dioxo-2,3-dihydro-1H-benzo[de]isoquinolin-6-yl)piperazine-1-carboxylate (4f)*:** Yellow solid, yield 48.3%. ^{1}H NMR (400 MHz, DMSO-d_6) δ 8.68 (d, *J* = 8.5 Hz, 1H, H-Ar), 8.60 – 8.51 (m, 2H, H-Ar), 7.97 (t, *J* = 7.9 Hz, 1H, H-Ar), 6.83 (s, 1H, H-Ar), 6.78 (t, *J* = 6.8 Hz, 1H, H-Ar), 6.67 (d, *J* = 8.0 Hz, 1H, H-Ar), 5.96 (s, 2H, CH_2-2O), 4.23 – 4.13 (m, 2H, -CH_2), 3.66 (s, 4H, 2-CH_2), 3.19 (s, 4H, 2-CH_2), 2.86 – 2.77 (m, 2H, -CH_2), 1.46 (s, 9H, 3-CH_3).^{13}C NMR (100 MHz, DMSO-d_6) δ162.81(C=O), 161.69 (C=O), 153.98, 147.25, 147.10, 145.68, 142.27, 132.87, 132.36, 129.62, 129.13, 128.52, 126.38, 122.96, 121.90, 121.50, 117.70, 108.98, 108.18, 100.70 (C-2O), 79.30 (C-O), 51.07 (C-N), 41.25 (CH_2), 33.09 (CH_2), 28.03 (CH_3). HRMS (m/z) (ESI): $C_{30}H_{30}N_4O_8[M+1]^+$ calcd for: 575.2136, found: 575.1059.

***Benzyl 4-(2-(4-methoxybenzyl)-5-nitro-1,3-dioxo-2,3-dihydro-1H-benzo[de]isoquinolin-6-yl)piperazine-1-carbodithioate (5a)*:** Yellow solid, yield 42.1%. ^{1}H NMR (600 MHz, $CDCl_3$) δ 8.72 (t, *J* = 3.4 Hz, 2H, H-Ar), 8.54 (d, *J* = 8.4 Hz, 1H, H-Ar), 7.88 (t, *J* = 7.9 Hz, 1H, H-Ar), 7.49 (d, *J* = 8.6 Hz, 2H, H-Ar), 7.41 (d, *J* = 7.4 Hz, 2H, H-Ar), 7.34 (t, *J* = 7.4 Hz, 2H, H-Ar), 7.29 (d, *J* = 7.3 Hz, 1H, H-Ar), 6.82 (d, *J* = 8.7 Hz, 2H, H-Ar), 5.29 (s, 2H, -CH_2), 4.63 – 4.19 (m, 6H, 3-CH_2), 3.76 (s, 3H, -OCH_3), 3.40 (s, 4H, 2-CH_2).^{13}C NMR (150 MHz, $CDCl_3$) δ 198.23 (C=S), 163.46 (C=O), 162.35 (C=O), 159.22, 146.30, 143.86, 135.55, 133.67, 130.83, 130.60, 130.36,

129.86, 129.55, 129.12, 128.81, 128.51, 127.85, 127.19, 124.00, 119.61, 113.93, 55.37 (OCH_3), 50.90 (C-N), 43.32 (CH_2), 42.51 (C-S). HRMS (m/z) (ESI): $C_{32}H_{28}N4O_5S_2[M+1]^+$ calcd for: 613.1574, found: 613.1552.

***Benzyl 4-(2-(2-(dimethylamino)ethyl)-5-nitro-1,3-dioxo-2,3-dihydro-1H-benzo[de]isoquinolin-6-yl)piperazine-1-carbodithioate (5b)*:** Yellow solid, yield 49.3%. ^{1}H NMR (400 MHz, DMSO-d_6) δ 8.73 (d, *J* = 8.4 Hz, 1H, H-Ar), 8.65 – 8.48 (m, 2H, H-Ar), 7.98 (t, *J* = 7.8 Hz, 1H, H-Ar), 7.43 (d, *J* = 7.0 Hz, 2H, H-Ar), 7.37 – 7.19 (m, 3H, H-Ar), 4.59 (s, 4H, 2-CH_2), 4.30 (s, 2H, -CH_2), 4.18 – 4.05 (m, 2H, -CH_2), 3.32 (s, 4H, 2-CH_2), 2.50 (s, 2H, -CH_2), 2.20 (s, 6H, 2-CH_3).^{13}C NMR (100 MHz, DMSO-d_6) δ 195.74 (C=S), 162.89 (C=O), 161.77 (C=O), 146.31, 142.52, 136.02, 132.98, 131.70, 129.59, 129.25, 129.15, 128.63, 128.49, 127.43, 126.33, 122.94, 118.15, 56.31 (CH_3), 50.64 (C-N), 45.32 (CH_2), 40.91 (C-S), 37.69 (CH_2). HRMS (m/z) (ESI): $C_{28}H_{29}N_5O_4S_2[M+1]^+$ calcd for: 564.1734, found: 564.1711.

***Benzyl 4-(2-(2-hydroxyethyl)-5-nitro-1,3-dioxo-2,3-dihydro-1H-benzo[de]isoquinolin-6-yl)piperazine-1-carbodithioate (5c)*:** Yellow solid, yield 52.4%. ^{1}H NMR (600 MHz, $CDCl_3$) δ 8.72 (d, *J* = 7.1 Hz, 1H, H-Ar), 8.69 (s, 1H, H-Ar), 8.56 (d, *J* = 8.4 Hz, 1H, H-Ar), 7.90 (t, *J* = 7.9 Hz, 1H, H-Ar), 7.40 (d, *J* = 7.3 Hz, 2H, H-Ar), 7.33 (t, *J* = 7.4 Hz, 2H, H-Ar), 7.29 (d, *J* = 7.3 Hz, 1H, H-Ar), 4.66 – 4.19 (m, 8H, 4-CH_2), 3.95 (t, *J* = 5.3 Hz, 2H, -CH_2), 3.41 (s, 4H, 2-CH_2).^{13}C NMR (150 MHz, $CDCl_3$) δ 198.23 (C=S), 164.22 (C=O), 163.08 (C=O), 146.52, 143.74, 135.52, 133.77, 130.84, 130.39, 129.82, 129.52, 128.78, 128.55, 127.82, 127.31, 123.68, 119.16, 61.42 (CH_2-O), 50.94 (C-N), 42.95 (CH_2), 42.48 (C-S). HRMS (m/z) (ESI): $C_{26}H_{24}N_4O_5S_2[M+1]^+$ calcd for: 537.1261, found: 537.1245.

***Benzyl 4-(2-(2-(benzo[d][1,3]dioxol-5-yl)ethyl)-5-nitro-1,3-dioxo-2,3-dihydro-1H-benzo[de]isoquinolin-6-yl)piperazine-1-carbodithioate (5d)*:** Yellow solid, yield 48.7%. ^{1}H NMR (600 MHz, $CDCl_3$) δ 8.76 – 8.69 (m, 2H, H-Ar), 8.59 (d, *J* = 8.4 Hz, 1H, H-Ar), 7.96 – 7.88 (m, 1H, H-Ar), 7.43 (d, *J* = 7.4 Hz, 2H, H-Ar), 7.36 (t, *J* = 7.5 Hz, 2H, H-Ar), 7.31 (d, *J* = 7.3 Hz, 1H, H-Ar), 6.84 (s, 1H, H-Ar), 6.80 – 6.72 (m, 2H, H-Ar), 5.94 (s, 2H, CH_2-2O), 4.80 – 4.07 (m, 8H, 4-CH_2), 3.44 (s, 4H, 2-CH_2), 2.98 – 2.87 (m, 2H, -CH_2).^{13}C NMR (150 MHz, $CDCl_3$) δ 198.21 (C=S), 163.26 (C=O), 162.10 (C=O), 147.75, 146.28, 143.83, 135.53, 133.50, 132.20, 130.60, 130.32, 129.88, 129.52, 128.78, 128.53, 127.82, 127.01, 123.86, 121.96, 119.46, 109.48, 108.40, 100.98 (C-2O), 50.87 (C-N), 42.48 (CH_2), 42.19 (C-S), 33.97 (CH_2). HRMS (m/z) (ESI): $C_{33}H_{28}N_4O_6S_2[M+1]^+$ calcd for: 641.1523, found: 641.1502.

***Benzyl 4-(2-(3,4-dihydroxyphenethyl)-5-nitro-1,3-dioxo-2,3-dihydro-1H-benzo[de]isoquinolin-6-yl)piperazine-1-carbodithioate (5e)*:** Yellow solid, yield 35.3%. ^{1}H NMR (600 MHz, DMSO-d_6) δ 8.85 – 8.71 (m, 3H), 8.61 – 8.50 (m, 2H, H-Ar), 8.02 – 7.93 (m, 1H, H-Ar), 7.43 (d, *J* = 7.3 Hz, 2H, H-Ar), 7.34 (t, *J* = 7.5 Hz, 2H, H-Ar), 7.28 (t, *J* = 7.3 Hz, 1H,

H-Ar), 6.67 – 6.57 (m, 2H, H-Ar), 6.47 (dd, *J* = 8.0, 1.9 Hz, 1H, H-Ar), 4.71 – 4.54 (m, 4H, 2-CH_2), 4.28 (s, 2H, -CH_2), 4.14 – 4.07 (m, 2H, -CH_2), 3.32 (s, 4H, 2-CH_2), 2.73 – 2.68 (m, 2H, -CH_2).^{13}C NMR (150 MHz, DMSO-d_6) δ 195.73 (C=S), 162.76 (C=O), 161.64 (C=O), 146.33, 145.21, 143.78, 142.45, 136.04, 132.96, 129.60, 129.31, 129.28, 129.11, 128.66, 128.54, 127.48, 126.29, 122.97, 119.24, 118.18, 115.97, 115.64, 50.70 (C-N), 45.55 (C-N), 41.56 (C-S), 40.96 (CH_2), 32.84 (CH_2). HRMS (m/z) (ESI): $C_{32}H_{28}N_4O_6S_2[M+1]^+$ calcd for: 629.1523, found: 629.1503.

***Benzyl 4-(5-nitro-1,3-dioxo-2-(phenylamino)-2,3-dihydro-1H-benzo[de]isoquinolin-6-yl)piperazine-1-carbodithioate (5f)*:**. Yellow solid, yield 38.1%.^{1}H NMR (400 MHz, DMSO-d_6) δ 8.82 (d, *J* = 8.3 Hz, 1H, H-Ar), 8.73 – 8.60 (m, 3H, H-Ar), 8.08 – 7.99 (m, 1H, H-Ar), 7.44 (d, *J* = 7.1 Hz, 2H, H-Ar), 7.37 – 7.25 (m, 3H, H-Ar), 7.14 (t, *J* = 7.9 Hz, 2H, H-Ar), 6.77 (t, *J* = 8.3 Hz, 3H, H-Ar), 4.72 – 4.23 (m, 6H, 3-CH_2), 3.51 – 3.35 (m, 4H, 2-CH_2).^{13}C NMR (100 MHz, DMSO-d_6) δ 195.74 (C=S), 162.44 (C=O), 161.37(C=O), 147.08, 146.61, 142.58, 136.02, 133.43, 132.11, 129.73, 129.38, 129.25, 128.79, 128.69, 128.49, 127.42, 126.81, 123.33, 119.52, 118.54, 112.53, 50.69 (C-N), 45.64 (C-N), 40.92 (C-S). HRMS (m/z) (ESI): $C_{30}H_{25}N_5O_4S_2[M+1]^+$ calcd for: 584.1421, found: 584.1400.

***Benzyl 4-(2-benzyl-5-nitro-1,3-dioxo-2,3-dihydro-1H-benzo[de]isoquinolin-6-yl)piperazine-1-carbodithioate (5g)*:** Yellow solid, yield 43.5%. ^{1}H NMR (600 MHz, $CDCl_3$) δ 8.74 (d, *J* = 7.0 Hz, 2H, H-Ar), 8.57 (d, *J* = 8.4 Hz, 1H, H-Ar), 7.93 – 7.88 (m, 1H, H-Ar), 7.54 (d, *J* = 7.4 Hz, 2H, H-Ar), 7.43 (d, *J* = 7.4 Hz, 2H, H-Ar), 7.36 (t, *J* = 7.5 Hz, 2H, H-Ar), 7.31 (q, *J* = 7.4 Hz, 3H, H-Ar), 7.29 – 7.26 (m, 1H, H-Ar), 5.37 (s, 2H, -CH_2), 4.75 – 4.21 (m, 6H, 3-CH_2), 3.43 (s, 4H, 2-CH_2).^{13}C NMR (150 MHz, $CDCl_3$) δ 198.20 (C=S), 163.42 (C=O), 162.32 (C=O), 146.34, 143.80, 136.82, 135.53, 133.71, 130.66, 130.35, 129.85, 129.52, 129.14, 128.78, 128.62, 128.51, 127.83, 127.82, 127.22, 123.90, 119.46, 50.89 (C-N), 43.86 (CH_2), 42.48 (C-S). HRMS (m/z) (ESI): $C_{31}H_{26}N_4O_4S_2$ $[M+1]^+$ calcd for: 583.1468, found: 583.1444.

***Benzyl 4-(2-(furan-2-ylmethyl)-5-nitro-1,3-dioxo-2,3-dihydro-1H-benzo[de]isoquinolin-6-yl)piperazine-1-carbodithioate (5h)*:** Yellow solid, yield 33.7%. ^{1}H NMR (600 MHz, DMSO-d_6) δ 8.75 (d, *J* = 8.5 Hz, 1H, H-Ar), 8.64 – 8.58 (m, 2H, H-Ar), 7.99 (t, *J* = 7.9 Hz, 1H, H-Ar), 7.55 – 7.51 (m, 1H, H-Ar), 7.43 (d, *J* = 7.4 Hz, 2H, H-Ar), 7.34 (t, *J* = 7.5 Hz, 2H, H-Ar), 7.28 (t, *J* = 7.3 Hz, 1H), 6.37 (dd, *J* = 8.0, 2.3 Hz, 2H), 5.22 (s, 2H, -CH_2), 4.65 – 4.52 (m, 4H, 2-CH_2), 4.29 (s, 2H, -CH_2), 3.34 – 3.26 (m, 4H, 2-CH_2).^{13}C NMR (150 MHz, DMSO-d_6) δ 195.72 (C=S), 162.60 (C=O), 161.49 (C=O), 149.98, 146.56, 142.47, 142.27, 136.02, 133.22, 131.99, 129.72, 129.30, 129.17, 128.67, 128.53, 127.47, 126.69, 122.80, 117.91, 110.61, 108.21, 50.73 (C-N), 40.94 (C-S), 36.34 (CH_2). HRMS (m/z) (ESI): $C_{29}H_{24}N_4O_5S_2[M+1]^+$ calcd for: 573.1261, found: 573.1237.

***Benzyl 4-(2-(4-chlorobenzyl)-5-nitro-1,3-dioxo-2,3-dihydro-1H-benzo[de]isoquinolin-6-yl)piperazine-1-carbodithioate (5i)*:** Yellow solid, yield 47.3%. ^{1}H NMR (400 MHz, DMSO-d_6) δ 8.76 (d, *J* = 8.8 Hz, 1H, H-Ar), 8.66 – 8.56 (m, 2H, H-Ar), 8.03 – 7.96 (m, 1H, H-Ar), 7.43 (d, *J* = 7.1 Hz, 2H, H-Ar), 7.39 – 7.32 (m, 6H, H-Ar), 7.29 (d, *J* = 7.2 Hz, 1H, H-Ar), 5.20 (s, 2H, -CH_2), 4.59 – 4.30 (m, 6H, 3-CH_2), 3.33 (s, 4H,2 -CH_2).^{13}C NMR (100 MHz, DMSO-d_6) δ 195.74 (C=S), 163.02 (C=O), 161.92 (C=O), 146.49, 142.53, 136.02, 133.18, 131.94, 131.73, 129.80, 129.51, 129.25, 129.16, 128.65, 128.49, 128.29, 127.43, 126.59, 122.90, 118.09, 50.68 (C-N), 42.45 (CH_2), 40.91 (C-S). HRMS (m/z) (ESI): $C_{31}H_{25}ClN_4O_4S_2[M+1]^+$ calcd for: 617.1079, found: 617.1059.

***6-(4-Benzoylpiperazin-1-yl)-2-(3-(methylamino)propyl)-5-nitro-1H-benzo[de]isoquinoline-1,3(2H)-dione (6a)*:** Yellow solid, yield 46.0%. ^{1}H NMR (400 MHz, DMSO-d_6) δ 8.66 (d, *J* = 8.5 Hz, 1H, H-Ar), 8.55 (s, 1H, H-Ar), 8.49 (s, 1H, H-Ar), 8.03 – 7.91 (m, 1H, H-Ar), 7.49 (s, 5H, H-Ar), 4.09 – 3.66 (m, 6H, 3-CH_2), 3.23 (d, *J* = 5.3 Hz, 5H), 3.03 – 2.87 (m, 2H, -CH_2), 2.51 (s, 3H, -CH_3), 2.04 – 1.91 (m, 2H, -CH_2).^{13}C NMR (100 MHz, DMSO-d_6) δ 169.54 (C=O), 163.07 (C=O), 161.97 (C=O), 146.81, 142.18, 135.59, 132.85, 131.55, 129.76, 129.60, 128.93, 128.57, 127.08, 126.24, 122.94, 117.76, 51.36 (C-N), 46.07 (CH_2), 37.20 (CH_3), 32.31 (CH_2), 24.30 (CH_2). HRMS (m/z) (ESI): $C_{27}H_{27}N_5O_5$ $[M+1]^+$ calcd for: 502.2085, found: 502.2064.

***6-(4-Benzoylpiperazin-1-yl)-2-(2-(dimethylamino)ethyl)-5-nitro-1H-benzo[de]isoquinoline-1,3(2H)-dione (6b)*:** Yellow solid, yield 45.1%. ^{1}H NMR (400 MHz, DMSO-d_6) δ 8.63 (d, *J* = 8.1 Hz, 1H, H-Ar), 8.52 (d, *J* = 7.2 Hz, 1H, H-Ar), 8.49 (s, 1H, H-Ar), 7.93 (dd, *J* = 8.4, 7.5 Hz, 1H, H-Ar), 7.49 (s, 5H, H-Ar), 4.08 (t, *J* = 6.8 Hz, 2H, -CH_2), 3.99 – 3.58 (m, 4H, 2-CH_2), 3.24 (s, 4H, 2-CH_2), 2.50 – 2.45 (m, 2H, -CH_2), 2.19 (s, 6H, 2-CH_3).^{13}C NMR (100 MHz, DMSO-d_6) δ 169.50 (C=O), 162.75 (C=O), 161.63 (C=O), 146.78, 142.20, 135.58, 132.82, 131.45, 129.69, 129.45, 128.99, 128.51, 128.44, 127.03, 126.34, 122.79, 117.59, 56.29 (CH_3), 51.25 (C-N), 45.33 (CH_2), 37.68 (CH_2). HRMS (m/z) (ESI): $C_{27}H_{27}N_5O_5[M+1]^+$ calcd for: 502.2085, found: 502.2073.

***6-(4-Benzoylpiperazin-1-yl)-2-(2-hydroxyethyl)-5-nitro-1H-benzo[de]isoquinoline-1,3(2H)-dione (6c)*:** Yellow solid, yield 53.2%. ^{1}H NMR (400 MHz, DMSO-d_6) δ 8.62 (d, *J* = 8.5 Hz, 1H, H-Ar), 8.50 (d, *J* = 7.2 Hz, 1H, H-Ar), 8.46 (s, 1H, H-Ar), 7.92 (t, *J* = 7.9 Hz, 1H, H-Ar), 7.49 (s, 5H, H-Ar), 4.80 (s, 1H, -OH), 4.07 (t, *J* = 6.4 Hz, 2H, -CH_2), 4.00 – 3.64 (m, 4H, 2-CH_2), 3.61 – 3.55 (m, 2H, -CH_2), 3.24 (s, 4H, 2-CH_2).^{13}C NMR (100 MHz, DMSO-d_6) δ 169.53 (C=O), 162.87 (C=O), 161.76 (C=O), 146.67, 142.17, 135.60, 132.71, 131.31, 129.71, 129.46, 128.91, 128.53, 128.43, 127.05, 126.16, 122.94, 117.77, 57.65 (CH_2), 51.29 (C-N), 41.92 (CH_2). HRMS (m/z) (ESI): $C_{25}H_{22}N_4O_6[M+1]^+$ calcd for: 475.1612, found: 475.1611.

***6-(4-Benzoylpiperazin-1-yl)-2-(4-chlorobenzyl)-5-nitro-1H-benzo[de]isoquinoline-1,3(2H)-dione (6d)*:** Yellow solid, yield 46.6%. ^{1}H NMR (400 MHz, DMSO-d_6) δ 8.72 (d, *J* = 8.4 Hz, 1H,

H-Ar), 8.65 – 8.57 (m, 2H, H-Ar), 7.99 (dd, *J* = 8.3, 7.6 Hz, 1H, H-Ar), 7.49 (s, 5H, H-Ar), 7.36 (q, *J* = 8.7 Hz, 4H, H-Ar), 5.20 (s, 2H, -CH_2), 4.02 – 3.60 (m, 4H, 2-CH_2), 3.27 (s, 4H, 2-CH_2). ^{13}C NMR (100 MHz, DMSO-d_6) δ 169.52 (C=O), 163.03 (C=O), 161.92 (C=O), 147.03, 142.34, 136.04, 135.61, 133.11, 131.80, 131.73, 129.80, 129.70, 129.50, 129.14, 128.53, 128.29, 127.04, 126.68, 122.91, 117.69, 51.33 (C-N), 42.44 (CH_2). HRMS (m/z) (ESI): $C_{30}H_{23}ClN_4O_5[M+1]^+$ calcd for:555.1430, found: 555.1408.

***6-(4-Benzoylpiperazin-1-yl)-2-(3,4-dihydroxyphenethyl)-5-nitro-1H-benzo[de]isoquinoline-1, 3(2H)-dione (6e)*:** Yellow solid, yield 42.1%. ^{1}H NMR (400 MHz, DMSO-d_6) δ 8.79 (s, 1H, -OH), 8.65 (d, *J* = 7.8 Hz, 2H, H-Ar), 8.57 – 8.48 (m, 2H), 8.00 – 7.90 (m, 1H, H-Ar), 7.49 (s, 5H, H-Ar), 6.63 (dd, *J* = 9.9, 5.0 Hz, 2H, H-Ar), 6.46 (dd, *J* = 8.0, 1.9 Hz, 1H, H-Ar), 4.15 – 4.06 (m, 2H, -CH_2), 3.94 – 3.70 (m, 4H, 2-CH_2), 3.25 (s, 4H, 2-CH_2), 2.75 – 2.63 (m, 2H, -CH_2).^{13}C NMR (100 MHz, DMSO-d_6) δ 169.52 (C=O), 162.67 (C=O), 161.55 (C=O), 146.82, 145.16, 143.73, 142.21, 135.61, 132.80, 131.47, 129.71, 129.51, 129.27, 129.02, 128.54, 128.48, 127.05, 126.29, 122.88, 119.21, 117.69, 115.94, 115.59, 51.30 (C-N), 41.48 (CH_2), 32.79 (CH_2). HRMS (m/z) (ESI): $C_{31}H_{26}N_4O_7[M+1]^+$ calcd for:567.1874, found: 567.1860.

***2-(4-Methoxybenzyl)-5-nitro-6-(4-tosylpiperazin-1-yl)-1H-benzo[de]isoquinoline-1,3(2H)-dio ne (7a)*:** Yellow solid, yield 34.2%. ^{1}H NMR (600 MHz, $CDCl_3$) δ 8.67 (s, 2H, H-Ar), 8.34 (d, *J* = 8.5 Hz, 1H, H-Ar), 7.78 (t, *J* = 7.8 Hz, 1H, H-Ar), 7.74 (d, *J* = 8.1 Hz, 2H, H-Ar), 7.48 (d, *J* = 8.5 Hz, 2H, H-Ar), 7.42 (d, *J* = 8.0 Hz, 2H, H-Ar), 6.82 (d, *J* = 8.6 Hz, 2H, H-Ar), 5.27 (s, 2H, -CH_2), 3.76 (s, 3H, -OCH_3), 3.45 – 3.29 (m, 8H, 4-CH_2), 2.50 (s, 3H, -CH_3).^{13}C NMR (150 MHz, $CDCl_3$) δ 163.41 (C=O), 162.31 (C=O), 159.18, 146.55, 144.31, 133.48, 133.05, 130.79, 130.56, 130.19, 130.11, 129.69, 129.10, 128.77, 128.26, 127.93, 127.09, 123.86, 119.41, 113.88, 55.34 (OCH_3), 50.87 (C-N), 46.32 (C-N), 43.25 (CH_2), 21.77 (CH_3). HRMS (m/z) (ESI): $C_{31}H_{28}N_4O_7S[M+1]^+$ calcd for: 601.1751, found: 601.1741.

***2-(2-(Dimethylamino)ethyl)-5-nitro-6-(4-tosylpiperazin-1-yl)-1H-benzo[de]isoquinoline-1,3(2 H)-dione (7b)*:** Yellow solid, yield 62.7%. ^{1}H NMR (400 MHz, DMSO-d_6) δ 8.54 – 8.47 (m, 2H, H-Ar), 8.44 (d, *J* = 8.5 Hz, 1H, H-Ar), 7.88 (dd, *J* = 8.4, 7.5 Hz, 1H, H-Ar), 7.72 (d, *J* = 8.2 Hz, 2H, H-Ar), 7.51 (d, *J* = 8.1 Hz, 2H, H-Ar), 4.08 (t, *J* = 6.7 Hz, 2H, -CH_2), 3.27 (s, 8H, 4-CH_2), 2.52 (d, *J* = 6.8 Hz, 2H, -CH_2), 2.45 (s, 3H, -CH_3), 2.21 (s, 6H, 2-CH_3). ^{13}C NMR (100 MHz, DMSO-d_6) δ 162.78(C=O), 161.67(C=O), 146.43, 143.82, 142.72, 132.94, 132.81, 131.33, 130.06, 129.36, 128.94, 128.57, 127.51, 126.14, 122.79, 118.12, 56.21 (CH_2), 50.53 (C-N), 45.94 (C-N), 45.20 (CH_2), 37.54 (CH_3), 21.07 (CH_3). HRMS (m/z) (ESI): $C_{27}H_{29}N_5O_6S[M+1]^+$ calcd for: 552.1911, found: 552.1894.

***2-(2-Hydroxyethyl)-5-nitro-6-(4-tosylpiperazin-1-yl)-1H-benzo[de]isoquinoline-1,3(2H)-dione (7c)*:** Yellow solid, yield 57.9%. ^{1}H NMR (400 MHz, DMSO-d_6) δ 8.56 – 8.48 (m, 2H, H-Ar),

8.45 (d, *J* = 8.5 Hz, 1H, H-Ar), 7.94 – 7.81 (m, 1H, H-Ar), 7.72 (d, *J* = 8.2 Hz, 2H, H-Ar), 7.52 (d, *J* = 8.1 Hz, 2H, H-Ar), 4.78 (s, 1H, -OH), 4.08 (t, *J* = 6.4 Hz, 2H, -CH_2), 3.58 (q, *J* = 6.3 Hz, 2H, -CH_2), 3.27 (s, 8H, 4-CH_2), 2.45 (s, 3H, -CH_3).^{13}C NMR (100 MHz, DMSO-d_6) δ 162.93 (C=O), 161.82 (C=O), 146.30, 143.82, 142.76, 132.94, 132.70, 131.21, 130.07, 129.43, 128.92, 128.57, 127.52, 125.97, 123.03, 118.42, 57.63 (CH_2-O), 50.53 (C-N), 45.96 (C-N), 41.93 (CH_2), 21.08 (CH_3). HRMS (m/z) (ESI): $C_{25}H_{24}N_4O_7S[M+1]^+$ calcd for: 525.1438, found: 525.1420.

***2-(2-(Benzo[d][1,3]dioxol-5-yl)ethyl)-5-nitro-6-(4-tosylpiperazin-1-yl)-1H-benzo[de]isoquinoline-1,3(2H)-dione (7d)*:** Yellow solid, yield 64.3%. ^{1}H NMR (600 MHz, $CDCl_3$) δ 8.69 (t, *J* = 3.4 Hz, 2H, H-Ar), 8.38 (d, *J* = 8.4 Hz, 1H, H-Ar), 7.83 (t, *J* = 7.9 Hz, 1H, H-Ar), 7.76 (d, *J* = 8.1 Hz, 2H, H-Ar), 7.43 (d, *J* = 8.0 Hz, 2H, H-Ar), 6.85 (s, 1H, H-Ar), 6.78 –6.74 (m, 2H, H-Ar), 5.94 (s, 2H, CH_2-2O), 4.37 – 4.28 (m, 2H, -CH_2), 3.46 – 3.25 (m, 8H, 4-CH_2), 2.99 – 2.89 (m, 2H, -CH_2), 2.52 (s, 3H, -CH_3).^{13}C NMR (150 MHz, $CDCl_3$) δ 163.32 (C=O), 162.15 (C=O), 147.79, 146.56, 146.32, 144.33, 144.05, 133.39, 133.15, 132.23, 130.60, 130.26, 130.14, 129.82, 128.33, 127.98, 127.01, 123.85, 122.00, 119.44, 109.52, 108.43, 101.01 (C-2O), 50.92 (C-N), 46.35 (C-N), 42.22 (CH_2), 34.00 (CH_2), 21.81 (CH_3). HRMS (m/z) (ESI): $C_{32}H_{28}N_4O_8S[M+1]^+$ calcd for: 629.1701, found: 629.1676.

***2-(3,4-Dihydroxyphenethyl)-5-nitro-6-(4-tosylpiperazin-1-yl)-1H-benzo[de]isoquinoline-1,3(2H)-dione (7e)*:** Yellow solid, yield 54.7%. ^{1}H NMR (400 MHz, DMSO-d_6) δ 8.79 (s, 1H, -OH), 8.66 (s, 1H, -OH), 8.49 (d, *J* = 5.1 Hz, 2H, H-Ar), 8.43 (d, *J* = 8.5 Hz, 1H, H-Ar), 7.87 (dd, *J* = 8.3, 7.6 Hz, 1H, H-Ar), 7.71 (d, *J* = 8.2 Hz, 2H, H-Ar), 7.51 (d, *J* = 8.1 Hz, 2H, H-Ar), 6.61 (d, *J* = 8.2 Hz, 2H, H-Ar), 6.44 (dd, *J* = 8.0, 1.9 Hz, 1H, H-Ar), 4.10 – 3.99 (m, 2H, -CH_2), 3.27 (s, 8H, 4-CH_2), 2.73 – 2.60 (m, 2H, -CH_2), 2.45 (s, 3H, -CH_3).^{13}C NMR (100 MHz, DMSO-d_6) δ 162.59 (C=O), 161.47 (C=O), 146.41, 145.14, 143.82, 143.72, 142.71, 132.93, 132.74, 131.30, 130.07, 129.33, 129.23, 128.94, 128.58, 127.51, 126.05, 122.80, 119.18, 118.16, 115.90, 115.56, 50.54 (C-N), 45.94 (C-N), 41.45 (CH_2), 32.76 (CH_2), 21.08 (CH_3). HRMS (m/z) (ESI): $C_{31}H_{28}N_4O_8S[M+1]^+$ calcd for: 617.1701, found: 617.1675.

***5-Nitro-2-(phenylamino)-6-(4-tosylpiperazin-1-yl)-1H-benzo[de]isoquinoline-1,3(2H)-dione (7f)*:** Yellow solid, yield 45.1%. ^{1}H NMR (600 MHz, $CDCl_3$) δ 8.72 (d, *J* = 7.6 Hz, 1H, H-Ar), 8.41 (d, *J* = 8.3 Hz, 1H, H-Ar), 7.87 – 7.82 (m, 1H, H-Ar), 7.73 (d, *J* = 8.2 Hz, 2H, H-Ar), 7.41 (d, *J* = 8.0 Hz, 2H, H-Ar), 7.21 (t, *J* = 7.9 Hz, 2H, H-Ar), 6.95 (t, *J* = 7.4 Hz, 1H, H-Ar), 6.90 (s, 1H, H-Ar), 6.86 (d, *J* = 7.8 Hz, 2H, H-Ar), 3.41 –3.35 (m, 8H, 4-CH_2), 2.49 (s, 3H, -CH_3).^{13}C NMR (150 MHz, $CDCl_3$) δ 162.53 (C=O), 161.41 (C=O), 147.23, 145.92, 144.38, 143.89, 134.24, 133.05, 131.32, 130.14, 130.02, 129.97, 129.37, 128.45, 127.95, 127.89, 123.54, 122.77, 118.87, 115.10, 51.02 (C-N), 46.28 (C-N), 21.79 (CH_3). HRMS (m/z) (ESI): $C_{29}H_{25}N_5O_6S[M+1]^+$ calcd for: 572.1598, found: 572.1576.

***2-Butyl-5-nitro-6-(4-tosylpiperazin-1-yl)-1H-benzo[de]isoquinoline-1,3(2H)-dione (7g)*:** Yellow solid, yield 44.9%. ^{1}H NMR (600 MHz, $CDCl_3$) δ 8.68 – 8.62 (m, 2H, H-Ar), 8.34 (d, *J* = 8.3 Hz, 1H, H-Ar), 7.80 (d, *J* = 7.7 Hz, 1H, H-Ar), 7.72 (d, *J* = 8.2 Hz, 2H, H-Ar), 7.40 (d, *J* = 8.0 Hz, 2H, H-Ar), 4.16 – 4.07 (m, 2H, -CH_2), 3.41 – 3.24 (m, 8H, 4-CH_2), 2.49 (s, 3H, -CH_3), 1.71 – 1.61 (m, 2H, -CH_2), 1.44 – 1.35 (m, 2H, -CH_2), 0.95 (t, *J* = 7.4 Hz, 3H, -CH_3).^{13}C NMR (150 MHz, $CDCl_3$) δ 163.42 (C=O), 162.26 (C=O), 146.42, 144.31, 144.00, 133.31, 133.06, 130.47, 130.20, 130.11, 129.74, 128.29, 127.93, 126.87, 123.90, 119.54, 50.86 (C-N), 46.34 (C-N), 40.55 (CH_2), 30.21 (CH_3), 21.78 (CH_2), 20.41 (CH_2), 13.92 (CH_3). HRMS (m/z) (ESI): $C_{27}H_{28}N_4O_6S[M+1]^+$ calcd for: 537.1802, found: 537.1805.

***2-Benzyl-5-nitro-6-(4-tosylpiperazin-1-yl)-1H-benzo[de]isoquinoline-1,3(2H)-dione (7h)*:** Yellow solid, yield 61.4%. ^{1}H NMR (400 MHz, DMSO-d_6) δ 8.51 (t, *J* = 3.3 Hz, 2H, H-Ar), 8.44 (d, *J* = 8.4 Hz, 1H, H-Ar), 7.85 (dd, *J* = 8.3, 7.6 Hz, 1H, H-Ar), 7.71 (d, *J* = 8.2 Hz, 2H, H-Ar), 7.50 (d, *J* = 8.1 Hz, 2H, H-Ar), 7.32 – 7.20(m, 5H, H-Ar), 5.16 (s, 2H, -CH_2), 3.28 (s, 8H, 4-CH_2), 2.43 (s, 3H, -CH_3).^{13}C NMR (100 MHz, DMSO-d_6) δ 162.82 (C=O), 161.73 (C=O), 146.57, 143.80, 142.67, 136.90, 132.97, 132.90, 131.47, 130.04, 129.45, 128.92, 128.55, 128.29, 127.61, 127.50, 127.09, 126.39, 122.70, 117.96, 50.57 (C-N), 45.93 (C-N), 42.95 (CH_2), 21.05 (CH_3). HRMS (m/z) (ESI): $C_{30}H_{26}N_4O_6S[M+1]^+$ calcd for: 571.1646, found: 571.1630.

***2-(Furan-2-ylmethyl)-5-nitro-6-(4-tosylpiperazin-1-yl)-1H-benzo[de]isoquinoline-1,3(2H)-dione (7i)*:** Yellow solid, yield 39.2%. ^{1}H NMR (600 MHz, $CDCl_3$) δ 8.68 (d, *J* = 6.5 Hz, 2H, H-Ar), 8.34 (d, *J* = 8.4 Hz, 1H, H-Ar), 7.79 (t, *J* = 7.9 Hz, 1H, H-Ar), 7.72 (d, *J* = 8.1 Hz, 2H, H-Ar), 7.40 (d, *J* = 8.0 Hz, 2H, H-Ar), 7.30 (d, *J* = 0.9 Hz, 1H), 6.42 (d, *J* = 3.1 Hz, 1H), 6.28 (dd, *J* = 3.1, 1.8 Hz, 1H), 5.34 (s, 2H, -CH_2), 3.41 – 3.28 (m, 8H, 4-CH_2), 2.48 (s, 3H, -CH_3).^{13}C NMR (150 MHz, $CDCl_3$) δ 163.10 (C=O), 161.97 (C=O), 149.94, 146.68, 144.32, 143.93, 142.35, 133.65, 133.07, 130.73, 130.28, 130.12, 129.78, 128.30, 127.95, 127.25, 123.70, 119.23, 110.54, 109.58, 50.90 (C-N), 46.32 (C-N), 36.58 (CH_2), 21.78 (CH_3). HRMS (m/z) (ESI): $C_{28}H_{24}N_4O_7S[M+1]^+$ calcd for: 561.1438, found: 561.1430.

***2-(4-Chlorobenzyl)-5-nitro-6-(4-tosylpiperazin-1-yl)-1H-benzo[de]isoquinoline-1,3(2H)-dione (7j)*:** Yield 55.3%, yellow solid. ^{1}H NMR (400 MHz, DMSO-d_6) δ 8.54 (t, *J* = 3.4 Hz, 2H, H-Ar), 8.47 (d, *J* = 8.3 Hz, 1H, H-Ar), 7.93 – 7.85 (m, 1H, H-Ar), 7.71 (d, *J* = 8.2 Hz, 2H, H-Ar), 7.51 (d, *J* = 8.2 Hz, 2H, H-Ar), 7.32 (dd, *J* = 8.0, 5.7 Hz, 4H, H-Ar), 5.16 (s, 2H, -CH_2), 3.28 (s, 8H, 4-CH_2), 2.44 (s, 3H, -CH_3).^{13}C NMR (100 MHz, DMSO-d_6) δ 162.89 (C=O), 161.80 (C=O), 146.61, 143.80, 142.72, 135.95, 133.01, 132.92, 131.72, 131.57, 130.05, 129.55, 129.50, 128.97, 128.59, 128.25, 127.50, 126.41, 122.76, 118.05, 50.58 (C-N), 45.93 (C-N), 42.40 (CH_2), 21.06 (CH_3). HRMS (m/z) (ESI): $C_{30}H_{25}ClN_4O_6S[M+1]^+$ calcd for: 605.1256, found: 605.1235.

4.3. Biological assays

The biological experimental procedures including antiproliferative activity assay, gel electrophoresis experiment, cell cycle analysis, cell apoptosis study, comet assay and western blot assay were carried out according to our previous work[17, 27-30] and described in the Supplementary Data (Part 1).

4.4. Molecular docking

All the docking studies were carried out using Sybyl-X 2.0 on a windows workstation and described in the Supplementary Data (Part 1). The crystal structure of the DNA were retrieved from the RCSB Protein Data Bank (DNA: 452D) [31].

Notes. The authors declare no competing financial interest.

Acknowledgments. This study was supported by the Innovative Team & Outstanding Talent Program of Colleges and Universities in Guangxi (2017-38), Guangxi New Century Ten, Hundred and Thousand Talents Project ([2017]42), Guangxi Natural Science Foundation (Nos. 2016GXNSFAA380300, 2014GXNSFBA118050 and 2018GXNSFAA138165), Guangxi Key Laboratory of Agricultural Resources Chemistry and Biotechnology (2019KF02), and Middle-aged and Young Teachers' Basic Ability Promotion Project of Guangxi (2019KY0542).

References.

[1] L. H. Hurley, DNA and its associated processes as targets for cancer therapy, Nat. Rev. Cancer. 2 (2002) 188−200.

[2] A. Skladanowski, P. Bozko, M. Sabisz, DNA structure and integrity checkpoints during the cell cycle and their rolein drug targeting and sensitivity of tumor cells to anticancer treatment, Chem. Rev. 109 (2009) 2951–2973.

[3] M. O. Hengartner, The biochemistry of apoptosis, Nature. 407 (2000) 770−776.

[4] B. L. Bloodgood, N. Sharma, H. A. Browne, A. Z. Trepman, M. E. Greenberg, The activity-dependent transcription factor NPAS4 regulates domain-specific inhibition, Nature. 503 (2013) 121−125.

[5] S. Banerjee, E. B. Veale, C. M. Phelan, S. A. Murphy, G. M. Tocci, L. J. Gillespie, D. O.; Kelly, J. M. Frimannsson, T. Gunnlaugsson, Recent advances in the development of 1, 8-naphthalimide

based DNA targeting binders, anticancer and fluorescent cellular imaging agents, Chem. Soc. Rev. 42 (2013) 1601–1618.

[6] M. Lv, H. Xu, Overview of naphthalimide analogs as anticancer agents, Curr. Med. Chem. 16(2009) 4797–4813.

[7] M. F. Braña, A. Ramos, Naphthalimides as anticancer agents: synthesis and biological activity,Curr. Med. Chem. Anticancer Agents.1 (2001) 237−255.

[8] Z. Chen, Y. Xu, X. Qian, Naphthalimides and analogues as antitumor agents: a review on molecular design, bioactivity and mechanism of action, Chinese Chem. Lett. 12 (2018) 1741−1756.

[9] A. Kamal, N. R. Bolla; P. S. Srikanth, A. K. Srivastava, Naphthalimide derivatives with therapeutic characteristics: a patent review, Expert. Opin. Ther. Patents. 23 (2013) 299−317.

[10] M. D. Tomczyk, K. Z. Walczak, l,8-Naphthalimide based DNA intercalators and anticancer agents. a systematic review from 2007 to 2017, Eur. J. Med. Chem. 159 (2018) 393−422.

[11] S.-Y. Tan, D. -H. Sun, J. -K Liu, X. Sun, F.-S. Wu, Q. Li, Y. -Q Yang, J. -X. Liu, X. Wang, Z.Chen, H. -L. Li, X. -H. Qian, Y.-F. Xu,Antiproliferative and apoptosis-inducing activities of novel naphthalimide-cyclam conjugates through dual topoisomerase (topo) I/II inhibition,Bioorg. Med. Chem. 23 (2015) 5672−5680.

[12] L. Ingrassia, F. Lefranc, R. Kiss, T. Mijatovic,Naphthalimides and azo-nafides as promising anti-cancer agents. Curr. Med. Chem. 16 (2009) 1192–1213.

[13] B. K. Sinha, J. Strong, N. W. Gibson, B.Kalyanaraman, Mechanism of DNA strand breaks by mitonafide, an imide derivative of 3-nitro-1,8-naphthalic acid, Biochem. Pharmacol. 34 (1985) 3845−3852.

[14] A. Kamal, S. Azeeza, E. V. Bharathi, M. S. Malik, R. V. C. R. N. C. Shetti, Search for new and novel chemotherapeutics for the treatment of human malignancies. Mini. Rev. Med. Chem. 10 (2010) 405−35.

[15] S. -X. Hua, R. -Z. Huang, M. -Y. Ye, Y. -M. Pan, G. -Y. Yao, Y. Zhang, H. -S. Wang, Design, synthesis and in vitro evaluation of novel ursolic acid derivatives as potential anticancer agents, Eur. J. Med. Chem. 95 (2015) 435−452.

[16] R. -Z. Huang, S. -X. Hua, C. -Y. Wang, Y. -M. Pan, J. -M. Qin, Z. -Y. Ding, Y. Zhang, H. -S. Wang, 4-Methylumbelliferones analogues as anticancer agents: synthesis and in cell pharmacological studies, Anti-Cancer Agents in Med. Chem.17 (2017) 576-589.

[17] M. Xin, J. -H. Wei, C. -H. Yang, G. -B. Liang, D. Su, X. -L. Ma, Y. Zhang, Design, synthesis and biological evaluation of 3-nitro-1,8-naphthalimides as potential antitumor agents, Bioorg.& Med. Chem. Lett. 30 (2020) 7051

[18] C. -S. Li, L. Belair, J. Guay, R. Murgasva, W. Sturkenboom, Y. K. Ramtohul, L. Zhang, Z. Huang, Thiazole analog as stearoyl-CoA desaturase 1 inhibitor, Bioorg.& Med. Chem. Lett. 19 (2009) 5214–5217.

[19] H. C. Anitha, S. Sreenivasa, R. N. Mohan, C. Vivek, G. Shivaraja, Synthesis, characterization and pharmacological assessment of alkylated sulfonyl piperazines, Asian Journal of Pharmacy and Pharmacology, 3 (2017) 177−185.

[20] Technical guidelines for non-clinical research of cytotoxic antitumor drugs, State Food and Drug Administration, 2006.

[21] S. Hattab, L. Chouba, M. B. Kheder, T. Mahouachi, H. Boussetta, Cadmium- and copper-induced DNA damage in Pisumsativum roots and leaves as determined by the Comet assay, Plant Biosyst. 143 (2009) S6−S11.

[22] M. B. Kastan, J. Bartek, Cell-cycle checkpoints and cancer, Nature, 2004, 432, 316−322.

[23] R. Boutros, V. Lobjois, B. Ducommun, CDC25 phosphatases in cancer cells: key players? Good targets? Nat. Rev. Cancer.7 (2007) 495−507.

[24] Y. Tsujimoto, J. Cossman, E. Jaffe, C. M. Croce, Involvement of the bcl-2 gene in human follicular lymphoma, Science, 228 (1985) 1440−1443.

[25] D. M. Hockenbery, M. Zutter, W. Hickey, M. Nahm, S. J. Korsmeyer, Bcl2 protein is topographically restricted in tissues characterized by apoptotic cell death, Proc. Natl. Acad. Sci. USA. 88 (1991) 6961−6965.

[26] S. Qiao, T. Nagasaka, T. Harada, N. Nakashima, p53, Bax and Bcl-2 expression, and apoptosis in gestational trophoblast of complete hydatidiform mole, Placenta. 19 (1998) 361−369.

[27]J. -H. Wei,Z.-F. Chen, J.-L. Qin, Y.-C. Liu, Z. Li, T. Khan, M.Wang, B. -P.Jiang, X. -C. Shen, H. Liang, Water-soluble oxoglaucine-Y(III), Dy(III) complexes: in vitro and in vivo anticancer activities by triggering DNA damage, leading to S phase arrest and apoptosis, Dalton T. 44 (2015) 11408−11419.

[28] G. -B. Liang, Y. -Y. Yu, J. -H. Wei, W. -B. Kuang, Z. -F. Chen, Y. Zhang, Design, synthesis and biological evaluation of naphthalenebenzimidizole platinum (II) complexes as potential antitumor agents, Eur. J. Med. Chem. 188 (2020) 112033.

[29] R. -Z. Huang, X. -T. Jing, X. -C. Huang, Y. -M. Pan, Y. -L. Fang, G. -B. Liang, Z. -X. Liao, H. -S. Wang, Z. -F. Chen, Y. Zhang, Bifunctional naphthoquinone aromatic amide-oxime derivatives exert combined immunotherapeutic and antitumor effects through simultaneous targeting of indoleamine-2, 3-dioxygenase and signal transducer and activator of transcription 3, J. Med. Chem. 63 (2020) 1544−1563.

[30] W. -B. Kuang, R. -Z. Huang, J. -L. Qin, X. Lu, Q. -P. Qin, B. -Q. Zou, Z. -F. Chen, H. Liang, Y. Zhang, Design, synthesis and pharmacological evaluation of new 3-(1Hbenzimidazol-2-yl)quinolin-2(1H)-one derivatives as potential antitumor agents, Eur. J. Med. Chem. 157 (2018) 139−150.

[31] A. K. Todd, A. Adams, J. H. Thorpe, W. A. Denny, L. P. G. Wakelin, C. J. Cardin, Major groove binding and 'DNA-induced' fit in the intercalation of a derivative of the mixed topoisomerase I/II poison N-(2-(dimethlyamino)ethyl)acridine-4-carboxamide (DACA) into DNA: X-ray structure complexed to d(CG(5Br-U)ACG)2 at 1.3-angstrom resolution. J. Med. Chem. 42 (1999) 536-540.

Tables

Table 1. *In vitro* antiproliferative activity of compounds **4**–**7**.

Figure Captions

Scheme 1. Synthetic route of the intermediate compounds *N*-substituted piperazines. Reagents and conditions: (a) CS_2, benzyl bromide, K_2CO_3, CH_2Cl_2, 0–5°C; (b) TFA, CH_2Cl_2, RT; (c) p-toluenesulfonyl chloride, RT; (d) benzoyl chloride, RT.

Scheme 2. Synthetic route of 3-nitro-1,4-naphthalimides derivatives **4**–**7**. Reagents and conditions: (a') HNO_3, HAc, 0–5°C; (b') *N*-substituted piperazines, 2-methoxyethanol, 110°C; (c') R-NH_2, ethanol, 80°C.

Fig. 1. Chemical structures of amonafide and mitonafide and their designed compounds.

Fig. 2. *In vivo* antitumor activity of compounds **6b** and **7b** in MGC-803 xenograft. (A) **6b** and **7b** (at 5 and 15 mg/kg doses), cisplatin (at 2 mg/kg dose), amonafide (at 5 mg/kg dose), or vehicle (5% DMSO in saline, v/v) was administered by intraperitoneal injection to inhibiting the tumor growth. Tumor growth was monitored by the mean tumor volume (mm^3) ± SD (n = 6) and calculated as the relative tumor increment rate (T/C, %). (B) Photographs of the harvested tumors from the mice. (C) Body weight change of the mice treated with compounds **6b** and **7b**. (D) Tumor weight of the mice. The tumors were collected in the mice at day 21. The "**" signs represent $p < 0.01$ (versus the vehicle control group)

Fig. 3. Gel electrophoresis assay results of pBR322 DNA treated with compounds **6b** and **7b**. R: linear form DNA, Sc: supercoiled form DNA, Nc: circular form DNA.

Fig. 4. Representative images of nuclei in the comet assay. MGC-803 cells were treated with 1.0 μM of compounds **6b** and **7b** for 24 h.

Fig. 5. Effect of compounds **6b** and **7b** on the expression levels of relevant proteins in MGC-803 cells line.

Fig. 6. Gel electrophoresis result of topoisomerase I treated with **6b** and **7b**. Compounds was added to the mixture of Topo I and pBR322 DNA; Lane 1and 9, pBR322 DNA + Topo I + CPT (5μM); Lane 2−6 and 10−14, pBR322 DNA + Topo I + **6a**/**7b**; Lane 7 and 15, pBR322 DNA + Topo I ; Lane 8 and16, pBR322 DNA only.

Fig. 7. Cell cycle analysis results of compounds **6b** and **7b** treated MGC-803 cells. MGC-803 cells were treated with compounds **6b** and **7b** at different concentrations (0, 0.25, 0.5 and 1 μM) for 24 h.

Fig. 8. Effect of compounds **6b** and **7b** on the expression levels of CDK2, cyclin E, and p21.

Fig. 9. Apoptosis ratio of the MGC-03 cells. MGC-803 cells were treated with compounds **6b** and **7b** at different concentrations (0, 0.5, 1 and 2 μM) for 24 h.

Fig. 10. The expression levels of Bax, Bcl-2, caspase-9, caspase-3 and PARP in the MGC-803 cells treated with compounds **6b** and **7b**.

Tables

Table 1. *In vitro* antiproliferative activity of compounds **4–7**.

Compd.	IC_{50}(μM)				
	SMMC-7721	T24	SKOV3	A549	MGC-803
4a	5.91±0.23	3.05±0.21	8.65±0.18	7.52±0.36	6.44±0.12
4b	1.05±0.09	0.83±0.15	0.65±0.13	1.08±0.15	1.33±0.23
4c	13.94±0.54	12.78±0.38	13.44±0.22	45.62±0.48	27.42±0.47
4d	7.76±0.35	9.52±0.32	12.67±0.43	40.37±0.50	16.10±0.41
4e	27.46±0.31	10.99±0.45	8.87±0.51	42.14±0.63	8.77±0.10
4f	14.38±0.33	9.71±0.38	7.48±0.35	16.51±0.22	25.16±0.21
5a	17.90±0.05	10.81±0.51	27.02±0.18	38.59±0.35	31.06±0.43
5b	3.17±0.09	2.06±0.13	2.40±0.18	1.98±0.11	6.08±0.21
5c	14.31±0.31	13.19±0.27	31.38±0.37	>50	15.40±0.53
5d	12.94±0.41	9.16±0.25	44.77±0.61	33.36±0.49	20.67±0.37
5e	22.47±0.27	10.71±0.13	26.26±0.31	17.36±0.21	25.43±0.53
5f	14.81±0.28	13.34±0.45	>50	>50	18.35±0.57
5g	13.51±0.32	13.13±0.34	34.20±0.41	>50	21.72±0.25
5h	11.64±0.31	18.35±0.22	40.35±0.63	44.52±0.48	21.16±0.25
5i	8.83±0.36	10.31±0.21	29.65±0.41	39.96±0.36	20.69±0.38
6a	4.73±0.24	4.65±0.17	4.11±0.31	6.66±0.23	8.22±0.32
6b	1.57±0.19	0.42±0.05	1.88±0.08	0.41±0.12	0.87±0.16
6c	11.99±0.43	9.93±0.56	16.81±0.42	31.33±0.51	12.88±0.43
6d	13.00±0.21	20.94±0.31	15.94±0.35	47.74±0.34	19.85±0.65
6e	19.72±0.24	14.56±0.25	19.91±0.14	22.53±0.42	9.31±0.16
7a	30.15±0.47	14.12±0.32	24.07±0.71	26.91±0.28	16.26±0.42
7b	2.71±0.13	0.33±0.07	0.32±0.03	0.27±0.15	1.42±0.11
7c	15.79±0.18	6.80±0.14	12.24±0.57	20.77±0.29	15.99±0.37
7d	16.60±0.34	9.17±0.45	28.92±0.57	41.76±0.27	12.81±0.15
7e	12.28±0.55	11.38±0.29	20.43±0.17	24.68±0.41	21.80±0.28
7f	14.38±0.33	10.74±0.42	23.19±0.56	38.39±0.26	16.16±0.34
7g	12.48±0.45	10.92±0.39	33.62±0.45	36.84±0.43	21.31±0.31
7h	14.85±0.35	12.66±0.26	38.16±0.56	42.91±0.69	10.78±0.24
7i	14.68±0.18	8.43±0.39	29.52±0.34	47.20±0.62	29.92±0.28
7j	17.59±0.72	6.37±0.21	30.39±0.51	>50	28.93±0.52
5-FU	15.32±0.67	40.14±2.14	26.34±0.57	34.47±1.90	34.85±1.75
Mitonafide	3.22±0.26	1.11±0.15	1.38±0.19	0.012±0.01	6.80±0.45
Amonafide	6.93±0.26	5.01±0.17	6.31±0.36	7.94±0.21	9.06±0.35

[α]IC_{50} values are presented as mean ± SD (standard error of the mean) from three repeating experiments.

Figures

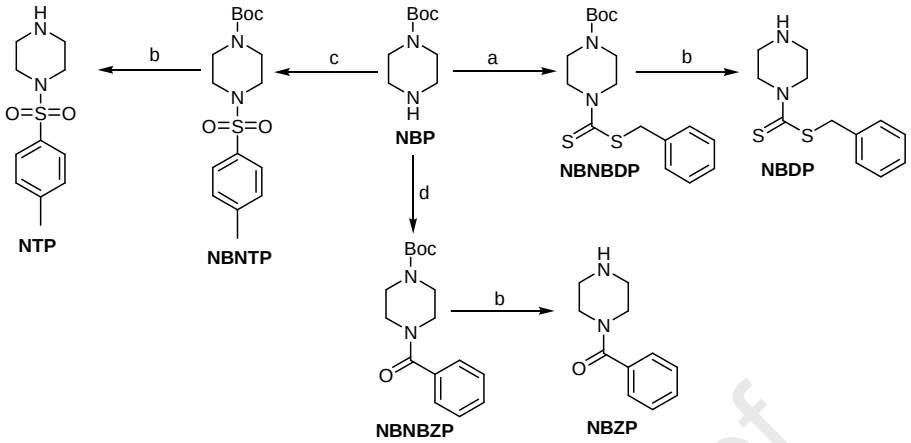

Scheme 1. Synthetic route of the intermediate compounds *N*-substituted piperazines. Reagents and conditions: (a) CS_2, benzyl bromide, K_2CO_3, CH_2Cl_2, 0–5°C; (b) TFA, CH_2Cl_2, RT; (c) p-toluenesulfonyl chloride, RT; (d) benzoyl chloride, RT.

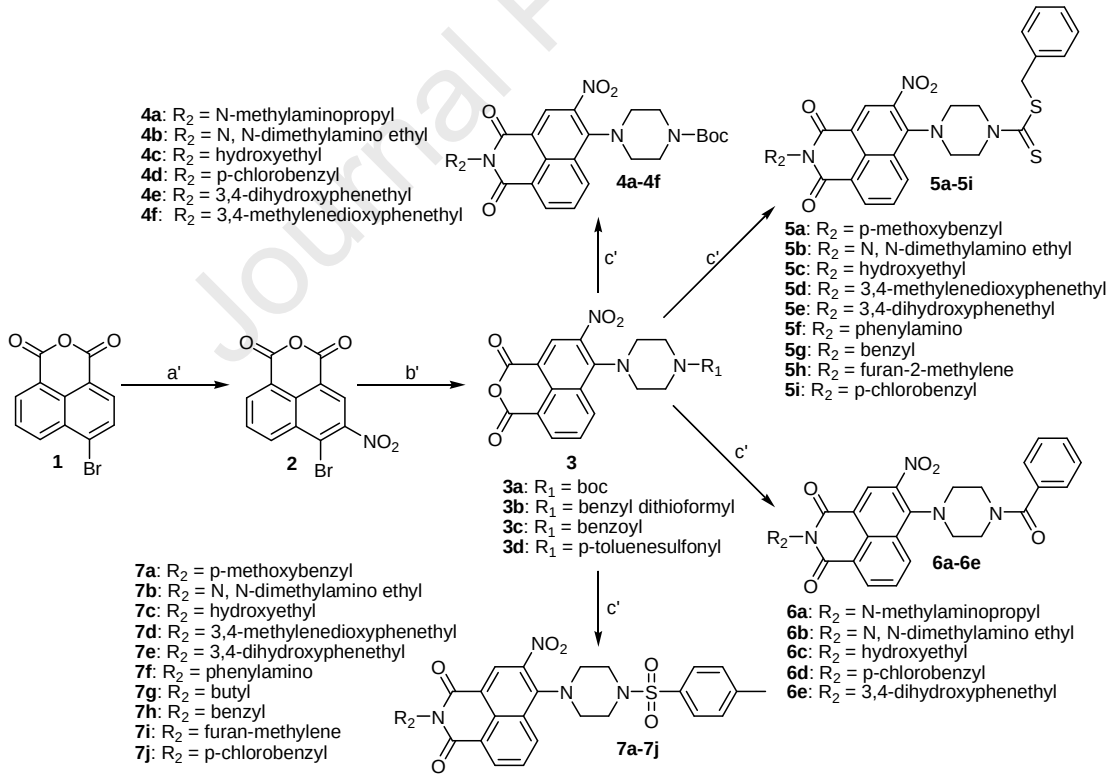

Scheme 2. Synthetic route of 3-nitro-1,4-naphthalimides derivatives **4**–**7**. Reagents and conditions:

(a') HNO_3, HAc, 0–5°C; (b') *N*-substituted piperazines, 2-methoxyethanol, 110°C; (c') R-NH_2, ethanol, 80°C.

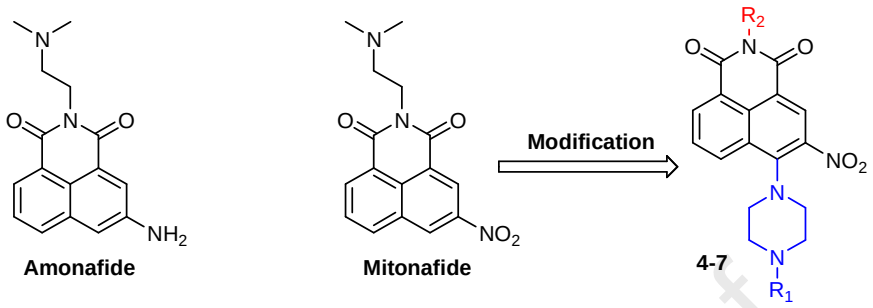

Fig. 1. Chemical structures of amonafide and mitonafide and their designed compounds.

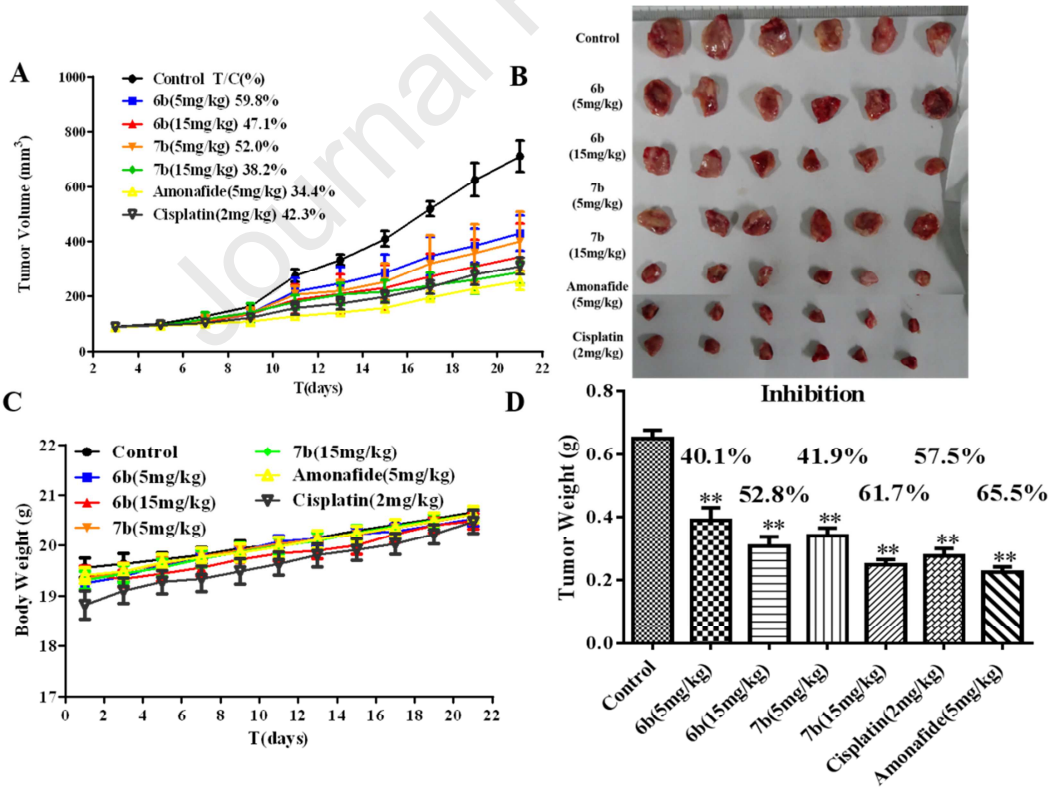

Fig. 2. *In vivo* antitumor activity of compounds **6b** and **7b** in MGC-803 xenograft. (A) **6b** and **7b** (at 5 and 15 mg/kg doses), cisplatin (at 2 mg/kg dose), amonafide (at 5 mg/kg dose), or vehicle

(5% DMSO in saline, v/v) was administered by intraperitoneal injection to inhibiting the tumor growth. Tumor growth was monitored by the mean tumor volume (mm^3) ± SD (n = 6) and calculated as the relative tumor increment rate (T/C, %). (B) Photographs of the harvested tumors from the mice. (C) Body weight change of the mice treated with compounds **6b** and **7b**. (D) Tumor weight of the mice. The tumors were collected in the mice at day 21. The "**" signs represent $p < 0.01$ (versus the vehicle control group).

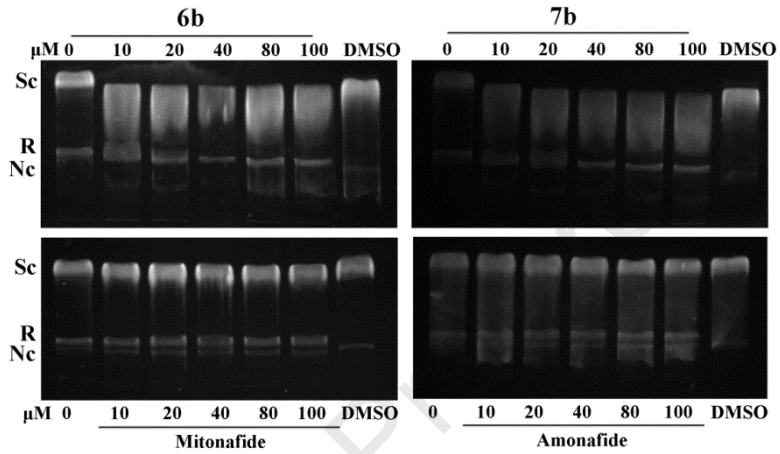

Fig. 3. Gel electrophoresis assay results of pBR322 DNA treated with compounds **6b** and **7b**. R: linear form DNA, Sc: supercoiled form DNA, Nc: circular form DNA.

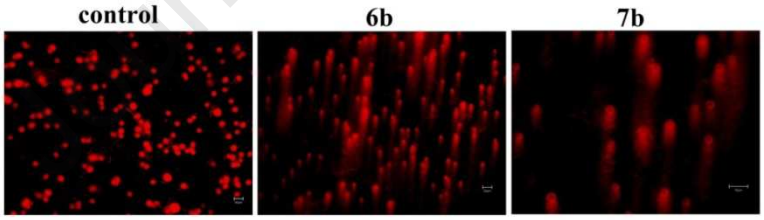

Fig. 4. Representative images of nuclei in the comet assay. MGC-803 cells were treated with 1.0 μM of compounds **6b** and **7b** for 24 h.

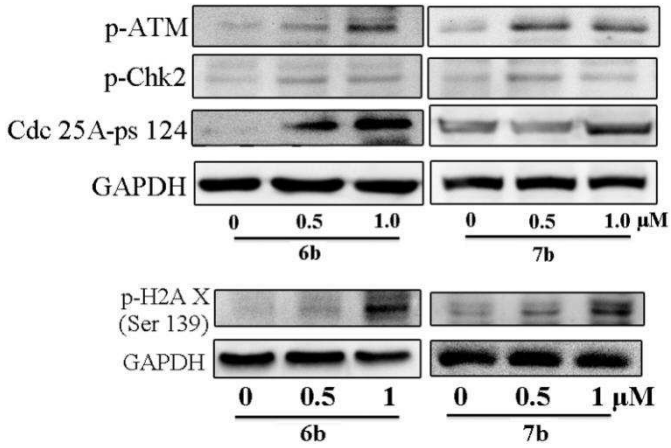

Fig. 5. Effect of compounds **6b** and **7b** on the expression levels of relevant proteins in MGC-803 cells line.

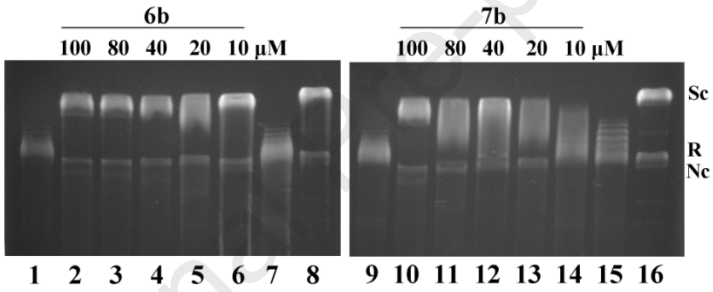

Fig. 6. Gel electrophoresis result of topoisomerase I treated with **6b** and **7b**. Compounds was added to the mixture of Topo I and pBR322 DNA; Lane 1and 9, pBR322 DNA + Topo I + CPT (5μM); Lane 2−6 and 10−14, pBR322 DNA + Topo I + **6a**/**7b**; Lane 7 and 15, pBR322 DNA + Topo I ; Lane 8 and16, pBR322 DNA only.

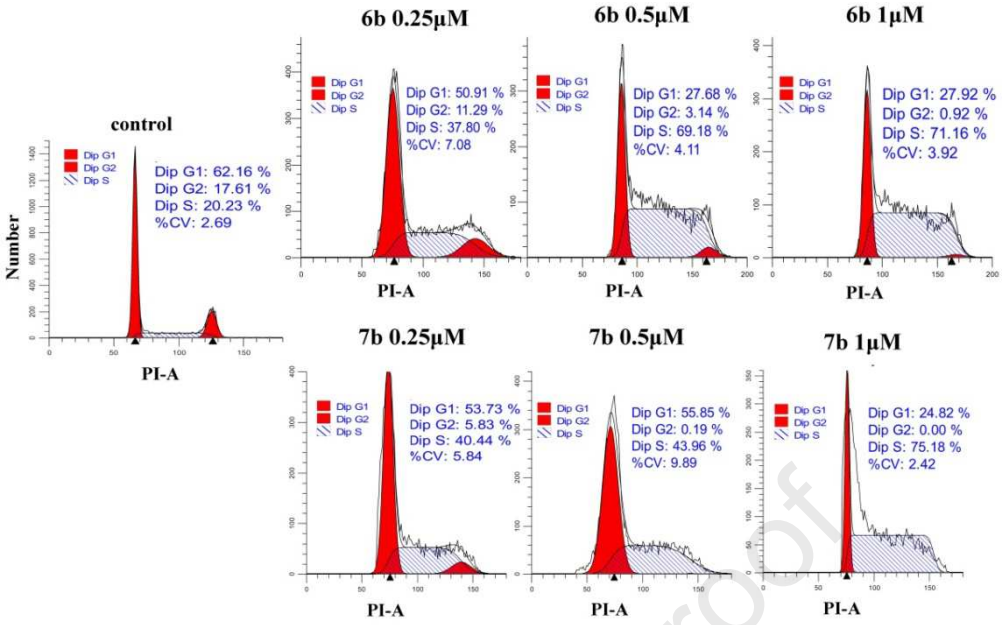

Fig. 7. Cell cycle analysis results of compounds **6b** and **7b** treated MGC-803 cells. MGC-803 cells were treated with compounds **6b** and **7b** at different concentrations (0, 0.25, 0.5 and 1 μM) for 24 h.

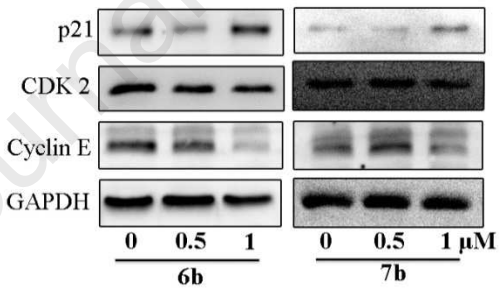

Fig. 8. Effect of compounds **6b** and **7b** on the expression levels of CDK2, cyclin E, and p21.

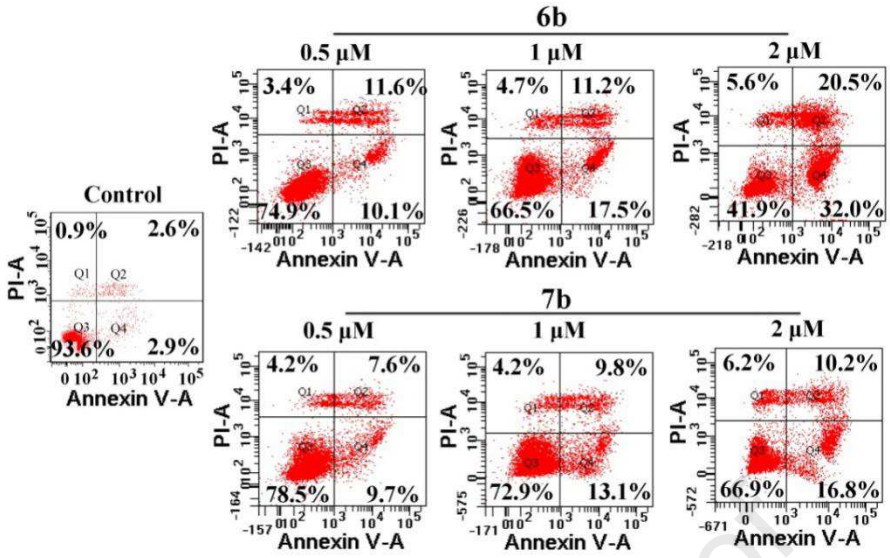

Fig. 9. Apoptosis ratio of the MGC-03 cells. MGC-803 cells were treated with compounds **6b** and **7b** at different concentrations (0, 0.5, 1 and 2 μM) for 24 h.

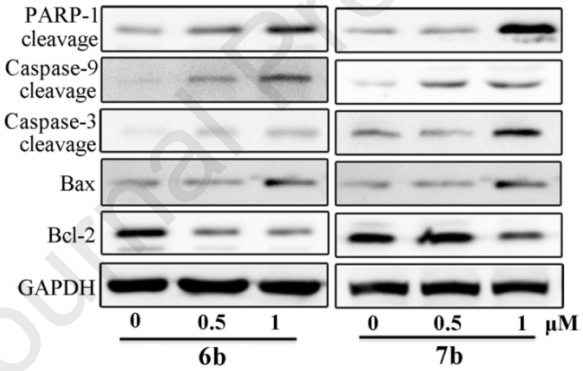

Fig. 10. The expression levels of Bax, Bcl-2, caspase-9, caspase-3 and PARP in the MGC-803 cells treated with compounds **6b** and **7b**.

Highlights

- Design, synthesis and antitumor evaluation of new 1,8-naphthalimides.
- *In vivo* antitumor activity screening for compounds **6b** and **7b**.
- Compounds **6b** and **7b** exhibited obvious DNA-targeting and topo 1-inhibition.
- Compounds **6b** and **7b** led to DNA-damage by regulation of related proteins.
- Compounds **6b** and **7b** induced cell cycle arrest and apoptosis.

Declaration of Interest Statement

We declare that we have no financial and personal relationships with other people or organizations that can inappropriately influence our work, there is no professional or other personal interest of any nature or kind in any product, service and/or company that could be construed as influencing the position presented in, or the review of, the manuscript entitled “Design, synthesis and antitumor evaluation of new 1,8-naphthalimide derivatives targeting nuclear DNA”.